1 **Microbial dynamics in a High-Arctic glacier forefield: a combined field, laboratory, and**

2 **modelling approach.**

3 James A. Bradley [1,2], Sandra Arndt [2], Marie Šabacká [1], Liane G. Benning [3,4], Gary L. Barker [5], Joshua

4 J. Blacker [3], Marian L. Yallop [5], Katherine E. Wright [1], Christopher M. Bellas [1], Jonathan Telling [1],

5 Martyn Tranter [1] , Alexandre M. Anesio [1]

7 [1] Bristol Glaciology Centre, School of Geographical Sciences, University of Bristol, BS8 1SS, UK

8 [2] BRIDGE, School of Geographical Sciences, University of Bristol, BS8 1SS, UK

9 [3] School of Earth and Environment, University of Leeds, LS2 9JT, UK

10 [4] GFZ, German Research Centre for Geosciences, 14473 Potsdam, Germany

11 [5] School of Biological Sciences, University of Bristol, BS8 1SS, UK

13 Corresponding author: James A. Bradley, email: j.bradley@bristol.ac.uk

15 **Abstract:** Modelling the development of soils in glacier forefields is necessary in order to assess how

16 microbial and geochemical processes interact and shape soil development in response to glacier

17 retreat. Furthermore, such models can help us predict microbial growth and the fate of Arctic soils in

18 an increasingly ice-free future. Here, for the first time, we combined field sampling with laboratory

19 analyses and numerical modelling to investigate microbial community dynamics in oligotrophic

20 proglacial soils in Svalbard. We measured low bacterial growth rates and growth efficiencies (relative

21 to estimates from Alpine glacier forefields), and high sensitivity to soil temperature (relative to

22 temperate soils). We used these laboratory measurements to inform parameter values in a new

23 numerical model and significantly refined predictions of microbial and biogeochemical dynamics of

24 soil development over a period of roughly 120 years. The model predicted the observed accumulation

25 of autotrophic and heterotrophic biomass. Genomic data indicated that initial microbial communities

26 were dominated by bacteria derived from the subglacial environment, whereas older soils hosted a

27 mixed community of autotrophic and heterotrophic bacteria. This finding was validated by the

28 numerical model, which showed that active microbial communities play key roles in fixing and

29 recycling carbon and nutrients. We also demonstrated the role of allochthonous carbon and microbial

30 necromass in sustaining a pool of organic material, despite high heterotrophic activity in older soils.

31 This combined field, laboratory and modelling approach demonstrates the value of integrated model-

32 data studies to understand and quantify the functioning of the microbial community in an emerging

33 High-Arctic soil ecosystem.

35 **Key words**

36 Glacier forefield

37 Microbial dynamics

38 Soil development

39 Numerical modelling

40 Integrated field-laboratory-modelling

1. Introduction

Polar regions are particularly sensitive to anthropogenic climate change (Lee, 2014) and have experienced accelerated warming in recent decades (Johannessen et al., 2004; Serreze et al., 2000; Moritz et al., 2002). The response of terrestrial Polar ecosystems to this warming is complex. Warmer conditions may increase soil respiration contributing to a positive feedback effect resulting from an increase in CO_2 efflux to the atmosphere. This will lead to further warming induced by the greenhouse effect (Billings, 1987; Oechel et al., 1993; Goulden et al., 1998). However, Arctic soils in particular may over several decades acclimatize to warming due to an increase in primary productivity, generating a net sink of CO_2 during the summer (Oechel et al., 2000). Accordingly, research to understand the response of terrestrial ecosystems in high latitudes to environmental change is of increasing importance. A visible consequence of Arctic warming is the large-scale retreat of glacier and ice cover (ACIA, 2005; Paul et al., 2011; Staines et al., 2014; Dyurgerov and Meier, 2000). From underneath the ice, a new terrestrial biosphere emerges, playing host to an ecosystem which may exert an important influence on biogeochemical cycles, and more specifically atmospheric CO_2 concentrations and associated climate feedbacks (Dessert et al., 2003; Anderson et al., 2000; Smittenberg et al., 2012; Berner et al., 1983). Furthermore, such a dramatic change will also invariably affect global methane budgets (Kirschke et al., 2013), the phosphorus cycle (Filippelli, 2002; Follmi et al., 2009) and the productivity of downstream and coastal ecosystems (Anesio et al., 2009; Mindl et al., 2007; Fountain et al., 2008; Anderson et al., 2000).

Numerous studies have attempted to characterize the physical and biological development of recently exposed soils using a chronosequence approach, whereby a transect perpendicular to the retreating ice snout represents a time sequence with older soils at increasing distance from the ice snout (Schulz et al., 2013). We have recently shown that microbial biomass and macronutrients (such as carbon, phosphorus and nitrogen) can accumulate in soils over timescales of decades to centuries (Bradley et al., 2014). In such pristine glacial forefield soils the activity of microbial communities is thought to be responsible for this initial accumulation of carbon and nutrients. Such an accumulation facilitates colonization by higher order plants, leading to the accumulation of substantial amounts of organic carbon (Insam and Haselwandter, 1989). However, organic carbon may also be derived from allochthonous sources such as material deposited on the soil surface (from wind, hydrology, precipitation and ornithogenic sources) and ancient organic pools derived from under the glacier (Schulz et al., 2013). Nevertheless, the relative significance of allochthonous and autochthonous sources of carbon to forefield soils, as well as their effect on ecosystem behavior are so far still poorly understood (Bradley et al., 2014). Moreover, cycling of bioavailable nitrogen (which is derived from active nitrogen-fixing organisms, allochthonous deposition, and degradation of organic substrates) and phosphorus (liberated from the weathering of minerals and decomposition of organic substrates) are similarly poorly quantified.

Several studies have observed shifts in the microbial community inhabiting pro-glacial soils of various ages (Zumsteg et al., 2012; Zumsteg et al., 2011). This was expressed in increasing rates of

81   autotrophic and bacterial production with soil age (Schmidt et al., 2008; Zumsteg et al., 2013;
82   Esperschutz et al., 2011; Frey et al., 2013) and the overall decline in quality of organic substrates in
83   older soils (Goransson et al., 2011; Insam and Haselwandter, 1989). However, current evidence is
84   limited to mostly descriptive approaches, which may be challenging to interpret due to inherent
85   difficulties in disentangling interacting microbial and geochemical processes across various temporal
86   and spatial scales. Furthermore, the inherent heterogeneity of glacial forefield soils makes the
87   development of a single conceptual model that fits all challenging. Accordingly, pro-glacial
88   biogeochemical processes that dominate such systems remain poorly quantified and highly under-
89   explored. This current lack of understanding limits our ability to predict the future evolution of these
90   emerging landscapes and the potential consequences on global climate. Numerical models present
91   an opportunity to expand our knowledge of glacier forefield ecosystems by analytically testing the
92   hypotheses that arise from observations, extrapolating, interpolating and budgeting processes, rates
93   and other features to explore beyond the possibility of empirical observation (Bradley et al., 2016).
94   With such a model we can then also explore the sensitivity and resilience of these ecosystems to
95   environmental change.
96
97   To address this, we have combined field observations, with laboratory incubations and elemental
98   measurements as well as genomic analyses and used these in a numerical model to investigate the
99   development of soils in a glacial forefield. With this data we refined some model parameters in the
100   recently developed *S*oil biogeoc*H*em*I*cal *M*odel for *M*icrobial *E*cosystem *R*esponse (SHIMMER 1.0;
101   Bradley et al. (2015)) model and applied this to the emerging forefield of the Midtre Lovénbreen
102   glacier in Svalbard. The Midtre Lovénbreen forefield is an ideal site to test the field-laboratory-model
103   approach due to the lack of vegetation during the first century of soil development, as this would
104   obscure the microbial community dynamics and considerably alter the physical properties of the soil
105   (Brown and Jumpponen, 2014; Ensign et al., 2006; King et al., 2008; Kastovska et al., 2005; Schutte
106   et al., 2009; Duc et al., 2009). The model development was informed by decades of empirical
107   research on glacier forefield soils, and has already been tested and validated using published
108   datasets from the Damma Glacier in Switzerland and the Athabasca Glacier in Canada. A thorough
109   sensitivity analysis highlighted the most important parameters to constrain in order to make further
110   predictions more robust. All our model parameter values are specific to individual, local model
111   conditions and inherently contain necessary model simplifications, abstractions and assumptions.
112   Nevertheless, our earlier sensitivity analyses revealed the following highly sensitive key parameters
113   as the most important to constrain through measurements: the maximum heterotrophic growth rate
114   (I_{maxH}), the bacterial growth efficiency (BGE, parameter Y_H) and the temperature response (Q_{10}).
115   Therefore, in this current study, we combined detailed field measurements with specifically designed
116   laboratory experiments and quantified values for these three parameters with a specific set of soils
117   from for the Midtre Lovénbreen forefield. With this data we have improved the confidence in our
118   model predictions and assessed the model performance. Finally, the model was used to explore
119   microbial community structure and carbon cycling dynamics in this High Arctic setting.
120

2. Methods

2.1. Study site and sampling

Midtre Lovénbreen is an Arctic polythermal valley glacier on the south side of Kongsfjorden, Western Svalbard (latitude 78°55'N, longitude 12°10'E) (Fig. 1). The Midtre Lovénbreen catchment is roughly 5 km East of Ny-Ålesund, where several long-term monitoring programs have provided a wealth of contextual information. Midtre Lovénbreen has experienced negative mass balance throughout much of the 20th century. Since the end of the Little Ice Age (maximum in Svalbard in the 1900s) the de-glaciated surface area of the Midtre Lovénbreen catchment has increased considerably in response to warming mean annual temperatures. This continues to the present day. Between 1966 and 1990 ~ 2.3 km^2 of land was exposed (Fleming et al., 1997; Moreau et al., 2008). We used a chronosequence approach to determine ages for soils based on satellite imagery (Landsat TM 7) and previously determined soil ages by aerial photography and carbon-14 dating techniques in Hodkinson et al. (2003). Soil samples were collected along a transect perpendicular to the glacier snout, representing soil ages of 0, 3, 5, 29, 50, and 113 years (Fig. 1) during the field season (18 July to 29 August 2013). At each of the 6 sites along the chronosequence, 10 meter traverses roughly parallel to the glacier snout were established and at each site 3 soil plots were sampled (using ethanol sterilized sampling equipment). After removing the > 2 cm rock pieces at each site, about 100 grams of soil was collected from the top 15 cm and immediately placed into sterile high-density polyethylene bags (Whirl-Pak (Lactun, Australia)) that were frozen and stored at -20°C, and transported to the laboratories in the Universities of Bristol and Leeds (UK).

2.2. Laboratory analyses

For bacterial abundance, samples were thawed and aliquots (100 mg) were immediately transferred into sterile 1.5 mL micro-centrifuge (Eppendorf) tubes, where they were diluted with 900 µL of Milli-Q water (0.2 µm filtered) and immediately fixed in 100 µL glutaraldehyde (0.2 µm filtered, 2.5% final concentration). Samples were then vortexed for 10 seconds and sonicated for 1 minute at 30°C to facilitate cell detachment from soil particles. Ten µL fluorochrome DAPI (4', 6-diamidino-2 phenylindole) was added to half of the samples, tubes were vortexed briefly (3 seconds) and incubated in the dark for 10 minutes, to be counted under UV light. The other half of each sample remained untreated, for counting under auto-fluorescent light for photosynthetic pigmentation. Samples were vortexed for 10 seconds and let stand for a further 30 seconds to ensure a well-mixed solution, prior to filtering 100 µL of the mixed liquid sample onto black Millipore Isopore membrane filters (0.2 µm pore size, 25 mm diameter), rinsed with a further 250 µL of Milli-Q water (0.2 µm filtered). Bacterial cells were then counted using an Olympus BX41 microscope at 1000 times magnification. The filtering apparatus was washed out with Milli-Q water between each filtration, and negative control samples, prepared using Milli-Q water, were included into each series. A negative control was a sample with no visible stained or auto-fluorescing cells. Thirty random grids (each 10^4 µm^2) were counted per sample. Cell morphologies were measured and cell volume was estimated and converted to carbon content according to Bratbak and Dundas (1984) (see Supplementary

160 Information). Separate aliquots of soil from each site were weighed after thawing and then dried at

161 105°C to obtain an estimate of soil moisture content.

162

163 Environmental DNA was isolated from at least 3 replicates for each soil age using MoBio PowerSoil®

164 DNA Isolation Kit and by following the instruction manual. The isolated 16S rDNA was amplified with

165 bacterial primers 515f (5'-GTGYCAGCMGCCGCGGTAA-3') and 926r (5'-

166 CCGYCAATTYMTTTRAGTTT-3'), creating a single amplicon of ~400 bp. The reaction was carried

167 out in 50 µL volumes containing 0.3 mg mL^{-1} Bovine Serum Albumin, 250 µM dTNPs, 0.5 µM of each

168 primer, 0.02 U Phusion High-Fidelity DNA Polymerase (Finnzymes OY, Espoo, Finland) and 5x

169 Phusion HF Buffer containing 1.5 mM MgCl$_2$. The following PCR conditions were used: initial

170 denaturation at 95°C for 5 minutes, followed by 25 cycles consisting of denaturation (95°C for 40

171 seconds), annealing (55°C for 2 minutes) and extension (72°C for 1 minute) and a final extension step

172 at 72°C for 7 minutes. Samples were sequenced using the Ion Torrent platform (using Ion 318v2 chip)

173 at Bristol Genomics facility at the University of Bristol. A non-barcoded library was prepared from the

174 amplicon pool using Life technologies Short Amplicon Prep Ion Plus Fragment Library Kit. The

175 template and sequencing kits used were: Ion PGM Template OT2 400 Kit and Ion PGM Sequencing

176 400 kit. The sequencing yielded 4.38 million reads. The 16S sequences were further processed using

177 MOTHUR (v. 1.35) and QIIME pipelines (Schloss et al., 2009; Caporaso et al., 2010). Chimeric

178 sequences were identified and removed using UCHIME (Edgar et al., 2011) and reads were clustered

179 into operational taxonomical units (OTUs), based on at least 97% sequence similarity, and assigned

180 taxonomical identification against Greengenes bacterial database (McDonald et al., 2012).

181

182 The carbon contents in the year 0 soils were analyzed with a Carlo-Erba elemental analyzer

183 (NC2500) at the German Research Center for Geosciences, Potsdam, Germany. The as-collected

184 soils were oven dried at 40°C for 48 hours, sieved to <7 mm and crushed using a TEMA disk mill to

185 achieve size fractions of < 20 µm. Total organic carbon (TOC) was analyzed after reacting the

186 powders with a 10% HCl solution for 12 hours to remove inorganic carbonates.

187

188 **2.3. Determination of maximum growth rates**

189 The microbial activity was determined in 113 year old soil samples after they were thawed (in the dark

190 at 5°C to mimic typical field temperature) for 168 hours. This age was chosen because these soil

191 samples were assumed to be the ones with the highest microbial biomass and activity and thus the

192 most appropriate for all laboratory measurements. Aliquots of the soils were divided into petri dishes

193 (25 g of soil (wet weight) into each petri dish) for subsequent treatments. In order to alleviate nutrient

194 limitations and measure maximum growth rates, four different nutrient conditions were simulated: (1)

195 no addition of nutrients, (2) low (0.03 mg C g^{-1}, 0.008 mg N g^{-1}, 0.02 mg P g^{-1}), (3) medium (0.8 mg C

196 g^{-1}, 0.015 mg N g^{-1}, 0.1 mg P g^{-1}) and (4) high additions (2.4 mg C g^{-1}, 0.024 mg N g^{-1}, 0.3 mg P g^{-1}).

197 The ranges and concentrations were informed by similar experiments in recently exposed proglacial

198 soils at the Damma Glacier, Switzerland (Goransson et al., 2011). Nutrients (C$_6$H$_{12}$O$_6$ for C, NH$_4$NO$_3$

199 for N and KH$_2$PO$_4$ for P) (Sigma, quality ≥99.0%) were dissolved in 2 mL Milli-Q water (0.2 µm

200   filtered), and mixed into the soils using an ethanol-sterilized spatula. Samples were incubated at 25°C

201   (for later comparison of growth rates with previous estimates (Frey et al., 2010)) in the dark for a

202   further 72 hours with the lids on. Throughout the whole incubation time, at 24 hour intervals, additional

203   2 mL aliquots of Milli-Q water (0.2 μm filtered) were added to maintain approximate soil moisture

204   conditions in each sample.

205

206   In these samples bacterial production was estimated by the incorporation of ^{3}H-leucine using the

207   microcentrifuge method detailed in Kirchman (2001). After the initial 72 hour incubation period

208   quadruplicate sample aliquots from the petri dish incubations and two trichloroacetic acid (TCA) killed

209   control samples were incubated for 3 hours at 25°C for every nutrient treatment. Approximately 50 mg

210   of soil was transferred to sterile micro-centrifuge tubes (2.0 mL, Fischer Scientific). Milli-Q (0.2 μm

211   pre-filtered) water and ^{3}H-leucine was added to a final concentration of 100 nM (optimum leucine

212   concentration was pre-determined by a saturation experiment, Fig. S1, Supplementary Information).

213   The incubation was terminated by the addition of TCA to each tube. Tubes were then centrifuged at

214   15,000 g for 15 minutes, the supernatant was aspirated with a sterile pipette and removed, and 1 ml

215   ice-cold 5% TCA was added to each tube. Tubes were then centrifuged again at 15,000g for 5

216   minutes, before again aspirating and removing the supernatant. 1mL ice-cold 80% ethanol was added

217   and tubes were centrifuged at 15,000 g for 5 minutes, before the supernatant was aspirated and

218   removed again and tubes were left to air dry for 12 hours. Finally, 1 mL of scintillation cocktail was

219   added, samples were vortexed, and then counted by liquid scintillation (Perkin Elmer Liquid

220   Scintillation Analyzer, Tri-Carb 2810 TR). Radioisotope activity of TCA-killed control samples was

221   always less than 1.1% of the measured activity in live samples. There was a positive correlation

222   between the amount of sediment added to the tubes and background counts representing

223   disintegrations per minute (DPM). Counts were individually normalized by the amount of sediments

224   (corrected for dry weight) used in each sample to discount for background DPM. Leucine

225   incorporation rates were converted into bacterial carbon production following the methodology of

226   Simon and Azam (1989). Bacterial abundance was estimated from each treatment after the 72 hour

227   incubation period by microscopy. Five samples from each petri dish were counted for each nutrient

228   treatment with negative controls yielding no detectable cells. One-way ANOVA (with post-hoc Tukey

229   HSD) statistical tests were used for evaluations of the variability from the multiple treatments.

230

231   **2.4. Temperature response**

232   Microbial community respiration was determined by measuring CO_2 gas exchange rates in airtight

233   incubation vials. Soil samples from the 113 year old site were defrosted and divided (25 g wet weight)

234   in petri dishes as above, and 2 mL of Milli-Q water (0.2 μm filtered) was added (to maintain

235   consistency of soil moisture with determination of bacterial production above). Samples were

236   incubated at 5°C (T_1) and 25°C (T_2) in the dark for a further 72 hours. 2mL of 0.2 μm pre-filtered Milli-

237   Q water was added to the T_1 sample (3 mL for T_2) at 24, 48 and 72 hours to maintain approximate soil

238   moisture content. Two separate killed control tests (one furnaced at 450°C for 4 hours, and one

239   autoclaved (3 cycles at 121°C)) were incubated at T_1 and T_2. Quintuple live and killed samples

240 (roughly 1 g) were transferred into cleaned 20 mL glass vials (rinsed in 2% Decon, submersed in 10%

241 HCl for 24 hours, rinsed 3 times with Milli-Q water and furnaced at 450°C for 4 hours). These were

242 sealed (9°C, atmospheric pressure, ambient CO_2 of 405 ppm) with pre-sterilized Bellco butyl stoppers

243 (pre-sterilized by boiling for 4 hours in 1M sodium hydroxide) and crimped shut with aluminum caps.

244 Sealed vials were then incubated at T_1 and T_2 for 24 hours in darkness. After 24 hours, the

245 headspace gas was removed with a gas-tight syringe and immediately analyzed on an EGM4 gas

246 analyzer (PP Systems, calibrated using gas standards matching the expected range, precision 1.9%,

247 2*SE). Empty pre-sterilized vials were also incubated and analyzed. Following gas analysis, vials

248 were opened and dried to a constant weight at 105°C to estimate moisture content and thus dry soil

249 weight of these aliquots. Headspace CO_2 change (ppm) was converted to microbial respiration using

250 the ideal gas law (n=PV/RT), assuming negligible changes in soil pore water pH (and therefore CO_2

251 solubility) during the incubation. CO_2 headspace changes resulting from killed controls and blanks

252 were < 70% of the changes resulting from the incubations at T_1, and <7% of the changes observed at

253 T_2. One-way ANOVA (with post-hoc Tukey HSD statistical tests) were used for comparison of multiple

254 treatments. No significant differences in CO_2 headspace change between killed controls at T_1 and T_2

255 were detected (P>0.05).

256

257 **2.5. Microbial Model: SHIMMER**

258 SHIMMER (Bradley et al., 2015) mechanistically describes and predicts transformations in carbon,

259 nitrogen and phosphorus through aggregated components of the microbial community as a system of

260 interlinked ordinary differential equations. The model is 0-D and represents the soil as a

261 homogeneous mix. Thus, light, temperature, nutrients, organic compounds and microbial biomass are

262 assumed to be evenly distributed. It categorizes microbes into autotrophs (A_{1-3}) and heterotrophs (H_{1-}

263 $_3$), and further subdivides these based on 3 specific functional traits. Microbes derived from

264 underneath the glacier (referred to as "subglacial microbes") are termed A_1 and H_1. A_1 are

265 chemolithoautotrophic, obtaining energy from the oxidation and reduction of inorganic compounds

266 and carbon from the fixation of carbon dioxide. In contrast, H_1 rely on the breakdown of organic

267 molecules for energy to support growth. A_2 and H_2 represent autotrophic and heterotrophic microbes

268 commonly found in glacier forefield soils with no "special" characteristics, and will be referred to as

269 "soil microbes". A_3 and H_3 are autotrophs and heterotrophs that are able to fix atmospheric N_2 gas as

270 a source of nitrogen in cases when dissolved inorganic nitrogen (DIN) stocks become limiting.

271 Available organic substrate is assumed to be derived naturally from dead organic matter and

272 allochthonous inputs. Labile compounds are immediately available fresh and highly reactive material,

273 rapidly turned over by the microorganisms (S_1, ON_1, OP_1). Refractory compounds are less

274 bioavailable and represents the bulk of substrate present in the non-living organic component of soil

275 (S_2, ON_2, OP_2).

276

277 Microbial biomass responds dynamically to changing substrate and nutrient availability (expressed as

278 Monod-kinetics), as well as changing environmental conditions (such as temperature and light). A Q_{10}

279 temperature response function (T_f) is affixed to all metabolic processes including growth rates and

280 death rates (Bradley et al., 2015), thus effectively slowing down or speeding up all life processes as

281 temperature changes (Soetaert and Herman, 2009; Yoshitake et al., 2010; Schipper et al., 2014).

282 Light limitation is expressed as Monod kinetics.

283

284 The following external forcings drive and regulate the system's dynamics:

285 • Photosynthetically-active radiation (PAR) (wavelength of approximately 400 to 700 nm) (W m^{-2}).

287 • Snow depth (m).

288 • Soil temperature (°C).

289 • Allochthonous inputs (μg g^{-1} day^{-1}).

290

291 Soil temperature (at 1 cm depth) for the entire of 2013 is provided by Alfred Wegener Institute for

292 Polar and Marine Research (AWI) from the permafrost observatory near Ny-Ålesund, Svalbard.

293 Similarly, PAR for 2013 are measured at the AWI surface radiation station near Ny-Ålesund,

294 Svalbard. Averaged daily snow depth for 2009 to 2013 is provided by the Norwegian Meteorological

295 Institute (eKlima). Allochthonous nutrient fluxes (inputs and leaching) are estimated based on an

296 evaluation of nutrient budgets of the Midtre Lovénbreen catchment (Hodson et al., 2005) in which

297 budgets for nutrient deposition rates and runoff concentrations are measured over two full summer-

298 winter seasons and residual retention rates (excess of inputs) or depletion rates (excess of outputs)

299 are inferred.

300

301 Initial conditions were informed by analysis of 0-years-of-exposure soil collected adjacent to the ice

302 snout, and initial values for all state variables are presented in Table 1. Initial microbial biomass was

303 estimated by microscopy as described above. Initial community structure was derived by 16S analysis

304 of year-0 soils. An initial value for carbon substrate (S1 + S2) was estimated based on the average

305 TOC content of year-0 soil. Bioavailability of model TOC was assumed to be 30% labile (S_1) and 70%

306 refractory (S_2) (for consistency with Bradley et al. (2015)). Organic nitrogen (ON) and organic

307 phosphorus (OP) were assumed to be stoichiometrically linked by the measured C:N:P ratio from the

308 Damma Glacier forefield (from which the model was initially developed and tested (Bradley et al.,

309 2015)). An initial value for DIN was taken from a previous evaluation of Svalbard tundra nitrogen

310 dynamics, whereby the lowest value is taken to represent the soil of least development, according to

311 traditional understanding of glacier forefields (Alves et al., 2013; Bradley et al., 2014). An initial value

312 for dissolved inorganic phosphorous (DIP) was established stoichiometrically from previous model

313 development and testing.

314

315 Model implementation and set-up is described in more detail in the Supplementary Information.

316

317 **2.6. Model parameters**

318 Maximum heterotrophic growth rate I_{maxH} (day^{-1}) was estimated by scaling the measured rate of

319 bacterial production (μg C g^{-1} day^{-1}) (converted to dry weight) with total heterotrophic biomass (μg C g^{-1}

320   ^{1}). Nutrient addition alleviates growth limitations as defined in SHIMMER (Bradley, 2015); thus

321   bacterial communities can be assumed to be growing at I_{maxH} under experimental conditions.

322

323   Y_H represents heterotrophic BGE, and was estimated according to the equation:

324

325
$$Y_H = \frac{BP}{BP + BR}$$

326   (1)

327   Where BP is and BR are measured bacterial production and measured bacterial respiration (µg C g^{-1}

328   day^{-1}) respectively, at 25°C with no nutrients added.

329

330   The temperature response (Q_{10}) value was estimated as:

331

332
$$Q_{10} = \left(\frac{R_2}{R_1}\right)^{\left(\frac{10}{T_2 - T_1}\right)}$$

333   (2)

334   Where R_1 and R_2 represent the measured respiration rate (µg C g^{-1} day^{-1}) at temperatures T_1 and T_2

335   (5°C and 25°C).

336

337   Laboratory-defined parameters (i.e. growth rate, temperature sensitivity and BGE) were assumed to

338   be the same for all microbial groups. A complete list of parameters and values is presented in Table

339   S3 (Supplementary Information).

340

341   **3. Results**

342   **3.1. Laboratory results and model parameters**

343   Bacterial production in untreated soil was estimated at 0.76 µg C g^{-1} day^{-1}, and across all nutrient

344   treatments ranged from 0.560 to 2.196 µg C g^{-1} day^{-1}. Nutrient addition led to increased measured

345   production (low = 0.69 µg C g^{-1} day^{-1}, medium = 1.09 µg C g^{-1} day^{-1}, high = 1.52 µg C g^{-1} day^{-1}),

346   however variability between replicates was also high and production rates from each nutrient

347   treatment were not significantly different from untreated soil ($P > 0.05$). The increased bacterial

348   production was cross-correlated with quadruplicate measurements of biomass from each treatment,

349   and resulting growth rates for all treatments were within a narrow range (0.359 to 0.550 day^{-1}) and

350   there was no statistically significant difference in growth rates between each nutrient treatment (Fig.

351   2b) ($P < 0.05$). The maximum measured growth rate for a single nutrient treatment, thus equating to

352   the parameter I_{maxH}, was 0.55 day^{-1}. The 95% confidence range for I_{maxH} is 0.50 to 0.60 day^{-1}. For

353   respiration, significantly higher CO_2 headspace concentration were detected in the live incubations at

354   25°C relative to killed controls ($P < 0.05$). Average respiration rate at 5°C was 1.61 C g^{-1} day^{-1} and

355   there was a significant increase in soil respiration at 25°C (12.83 µg C g^{-1} day^{-1}) (Fig. 2c) ($P < 0.05$).

356   The Q_{10} value for Midtre Lovénbreen forefield soils was thus calculated as 2.90, and a 95%

357   confidence range was established as 2.65 to 3.16. Based on measured values of bacterial production

358   and respiration, BGE (Y_H) was 0.06, with a 95% confidence range of 0.05 to 0.07. Final calculated

359   values for model parameters are summarized in Table S3 (Supplementary Information).

360

361   The results from microscopy determination of biomass are presented in Table 2. In the freshly

362   exposed soil (year 0) heterotrophic biomass was low (0.059 µg C g^{-1}), increased substantially to 0.244

363   µg C g^{-1} in 29 year old soils, and was an order or magnitude higher (2.00 µg C g^{-1}) in 113 year old

364   soils. Autotrophic biomass was considerably higher than heterotrophic biomass and increased by

365   roughly an order of magnitude from year 0 (0.171 µg C g^{-1}) to year 29 (1.07 µg C g^{-1}) and

366   approximately doubled by year 113 (2.58 µg C g^{-1}). TOC in freshly exposed soil was approximately

367   0.793 mg C g^{-1}).

368

369   16S data was categorized into microbial groups (A_{1-3} and H_{1-3}) as defined by the model formulation.

370   Chemolitotrophs, such as known iron or sulfur oxidizers (genera *Acidothiobacillus*, *Thiobacillus*,

371   *Gallionella*, *Sulfurimonas*) were assigned into the A_1 group. Phototrophic microorganisms, such as

372   cyanobacteria (*Phormidium*, *Leptolyngbya*) and phototrophic bacteria (*Rhodoferax*, *Erythrobacter*,

373   *Halomicronema*) were allocated into group A_2, while heterocyst forming, cyanobacteria from the

374   orders Nostocales and Stigonematales were assigned to group the A_3 (nitrogen-fixing autotrophs).

375   Members of the family Comamonadaceae of the Betaproteobacteria are known subglacial dwelling

376   microorganisms (Yde et al., 2010) and were thus included into the group H_1. General soil

377   heterotrophic microorganisms (mainly members of Alphaproteobacteria, Actinobacteria,

378   Bacterioidetes and Acidobacteria) were assigned into group H_2 (general soil heterotrophs). Lastly,

379   group H_3 consisted of heterotrophic nitrogen fixers, mainly *Azospirillum*, *Bradyrhizobium*, *Devosia*,

380   *Clostridium*, *Frankia* and *Rhizobium*. Pathogens, non-soil microorganisms and organisms with

381   unknown physiological traits were assigned into "Uncategorized" group. Subglacial microbes

382   accounted for 43 to 45 % of reads in year 0 and 5, and declined in older soils (year 50 and 113) to 18

383   to 22%. The subglacial community was predominantly chemolithoautotrophic (A_1). Typical soil

384   bacteria (A_2 and H_2) increased from low abundance (30% and 40% in years 0 and 5 respectively) to

385   relatively high abundance (63 to 67%) of reads in years 50 and 113. Nitrogen fixing bacteria were

386   prevalent in recently exposed soils (14% in year 0) but low in relative abundance in soils above 5

387   years of age (4 to 6% in years 5, 50 and 113). In the freshly exposed soil (year 0), the microbial

388   community was relatively evenly distributed between heterotrophs (43%) and autotrophs (44%). In

389   developed soils, the relative abundance of heterotrophs increased (up to 74% of reads in years 50

390   and 113). Important to note is the fact that between 8 and 21% of the reads across all samples could

391   not be classified.

392

393   **3.2. Model Results**

394   The model predicted an accumulation of autotrophic and heterotrophic biomass over 120 years (Fig.

395   3a and 3b). Biomass and nutrient concentrations were initially extremely low (total biomass < 0.25 µg

396   C g^{-1}, DIN < 4.0 µg N g^{-1}, DIP < 3.0 µg P g^{-1}), and biological activity in initial soils was also low (Table

397   3). There was an order of magnitude increase in total microbial biomass in years 10 to 60. Nitrogen-

398 fixing autotrophs (A_3) and heterotrophs (H_3), and soil heterotrophs (H_2) experienced rapid growth

399 during this period. Subglacial and soil autotrophs (A_{1-2}) and subglacial heterotrophs (H_1) remained

400 low. Bacterial production increased by roughly two orders of magnitude (Table 3). Organic carbon

401 (labile and refractory) increased (Fig. 3c), whilst DIN and DIP concentrations increased by

402 approximately an order of magnitude in the first 60 years (Fig. 3d). During the later stages of soil

403 development (years 60 to 120), biomass increased rapidly due to the rapid growth of soil organisms

404 (A_2 and H_2), which outcompeted nitrogen-fixers. The model showed a rapid exhaustion of labile

405 organic carbon (years 50 to 100), while refractory carbon accumulated slowly. Nutrients (DIN and

406 DIP) accumulated at a relatively constant rate. Microbial activity, including bacterial production,

407 nitrogen fixation and DIN assimilation, was high relative to early stages (Table 3).

408

409 A carbon budget of fluxes through the substrate pool is presented in Fig. 4. Daily fluxes are presented

410 in panels (a) for year 5, (b) for year 50 and (c) for year 113, and annual fluxes up to year 120 are

411 presented in (d). In recently exposed soils (5 years), allochthonous inputs were the only noticeable

412 carbon flux, outweighing heterotrophic growth and respiration, and the contribution of substrate from

413 necromass and exudates by over two orders of magnitude (Fig. 4a). Thus, the total change in carbon

414 (black line) closely resembled allochthonous input. In the intermediate stages (Fig. 4b), there was

415 substantial depletion from the substrate pool due to heterotrophic activity. Heterotrophic growth (red

416 line) was low despite high substrate consumption and respiration (orange line). In the late stages of

417 soil development, the flux of microbial necromass was a significant contributor to the organic

418 substrate pools (Fig. 4c). Carbon fluxes in mid to late stages of soil development were highly

419 seasonal (Fig. 4b and 4c). Biotic fluxes (e.g. respiration) were up to six times higher during the

420 summer (July to September) compared to the winter (November to April), however a base rate of

421 heterotrophic respiration and turnover of microbial biomass was sustained over winter. Figure 4d

422 shows that the contribution of microbial necromass rose steadily throughout the simulation (blue line),

423 however was not sufficient to compensate the uptake of carbon substrate, thus leading to overall

424 depletion between years 50 to 110 (black line). The contribution of exudates (green line) to substrate

425 was minimal at all soil ages.

426

427 **4. Discussion**

428 **4.1. Determination of parameters and model predictions**

429 The maximum microbial growth rate (I_{max}) was determined by incorporation of ^{3}H-leucine as 0.550

430 day^{-1}. This value is, to our knowledge, is the first measured rate of bacterial growth from High-Arctic

431 soils, and falls within the lower end of the plausible range established in Bradley et al. (2015) (0.24 –

432 4.80 day^{-1}) for soil microbes from a range of laboratory and modelling studies (Fig. 5a) (Frey et al.,

433 2010; Ingwersen et al., 2008; Knapp et al., 1983; Zelenev et al., 2000; Stapleton et al., 2005; Darrah,

434 1991; Blagodatsky et al., 1998; Vandewerf and Verstraete, 1987; Foereid and Yearsley, 2004; Toal et

435 al., 2000; Scott et al., 1995). Figure 6 illustrates the influence of the site-specific, laboratory-derived

436 parameters on microbial biomass predictions. It compares the range of predicted microbial biomass

437 based on laboratory-determined parameters (yellow) to the entire plausible parameter range (red;

438 Bradley et al. (2015)). Predicted biomass with the average laboratory-derived value is indicated by the

439 black line. For I_{max}, predicted biomass with laboratory-derived parameters (yellow shading) was

440 towards the lower end of the plausible range (Fig. 6a) because refined growth rates were significantly

441 lower than the maximum values explored previously. This was mostly due to a significant reduction in

442 autotrophic biomass (A_{1-3}). With high growth rates, there was a sharp early increase in biomass (years

443 10 to 20) followed by slower growth phase (years 20 to 120). Model results with laboratory-derived

444 growth rates showed that the exponential growth phase occurred later (years 40 to 80) and was more

445 prolonged, but total biomass was considerably lower. There was a substantial reduction in the

446 plausible range in predicted microbial biomass.

447

448 The laboratory-derived Q_{10} for Midtre Lovénbreen was at the upper end of the plausible range

449 previously identified in Bradley et al. (2015) (Fig. 5b). There was a substantial reduction in the

450 plausible range in predicted microbial biomass (Fig. 6b) from the measured temperature sensitivity

451 (yellow) compared to the previous range (red). Soil microbial communities in Polar regions must

452 contend with extremely harsh environmental conditions such as cold temperatures, frequent freeze-

453 thaw cycles, low water availability, low nutrient availability, high exposure to ultraviolet radiation in the

454 summer, and prolonged periods of darkness in winter. These factors profoundly impact their

455 metabolism and survival strategies and ultimately shape the structure of the microbial community

456 (Cary et al., 2010). High Q_{10} values, as derived here, are typical of cold environments and cold

457 adapted organisms and this has been associated with the survival of biomass under prolonged

458 periods of harsh environmental conditions (Schipper et al., 2014). An investigation into the

459 metabolism of microbial communities in biological soils crusts in recently exposed soils from the East

460 Brøgger Glacier, approximately 6 km from the Midtre Lovénbreen catchment, also derived a high Q_{10}

461 (3.1) (Yoshitake et al., 2010). The Midtre Lovénbreen catchment, in Svalbard, experiences a relatively

462 extreme Arctic climate. The high Q_{10} ultimately lowers the overall rate of biomass accumulation in

463 ultra-oligotrophic soils and a baseline population is maintained.

464

465 Measured BGE (Y_H) was 0.06 (Fig. 5c). The low BGE calculated here suggested that a high

466 proportion (94%) of substrate consumed by heterotrophs is recycled (degrading organic substrate into

467 DIC (CO_2), DIN and DIP), with very little being incorporated into biomass (6%). Low BGE encouraged

468 the liberation and release of nutrients to the soil and thus the overall growth response of the total

469 microbial biomass was more rapid due to higher soil nutrient concentrations (Fig. 6c). However, due

470 to the low BGE, there was a high rate of substrate degradation, and as such, labile substrate was

471 rapidly depleted when heterotrophic biomass was high (Fig. 3c). Heterotrophic growth requires that a

472 substantial amount of substrate is degraded – thus, although autotrophic production outweighed

473 heterotrophic production at all stages of development (Fig. 3e), the soil was predicted by the model to

474 be a net source of CO_2 to the atmosphere over the first 120 years of exposure (Fig. 3f). There are

475 very few measurements of BGE in cold glaciated environments, however previous studies have

476 suggested values as low as 0.0035 to 0.033 (Anesio et al., 2010; Hodson et al., 2007).

477

4.2. Microbial biomass dynamics and community structure

478

479 Measured microbial biomass in the initial soils of Midtre Lovénbreen (0.23 µg C g^{-1}, 0 years) was very

480 low compared to initial soils in other deglaciated forefields of equivalent ages in lower latitudes, for

481 example in the Alps (4 µg C g^{-1}) (Bernasconi et al., 2011; Tscherko et al., 2003) and Canada (6 µg C

482 g^{-1}) (Insam and Haselwandter, 1989). However, our microbial biomass values are more similar to

483 other recently deglaciated soils in Antarctica (Ecology Glacier - 0.88 µg C g^{-1}) (Zdanowski et al.,

484 2013). Low biomass is possibly a result of the harsh, ultra-oligotrophic and nutrient limiting

485 environment of the High Arctic and Antarctica, where low temperature and longer winters limit the

486 summer growth phase, especially compared to an Alpine system (Tscherko et al., 2003; Bernasconi

487 et al., 2011).

488

489 The initial microbial community structure in our samples was predominantly autotrophic (74.5%). In

490 the years following exposure, we observed an increase in autotrophs and heterotrophs with soil age

491 (Table 3), presumably due to the establishment and growth of stable soil microbial communities

492 (Schulz et al., 2013; Bradley et al., 2014). Both the observations and modelling results suggested that

493 there was no substantial increase in heterotrophic biomass during the initial and early-intermediate

494 stages of soil development (years 0 to 40), which was then followed by a growth phase whereby

495 biomass increased by roughly an order of magnitude. Overall, the model and the microscopy data

496 were in good agreement accounting for the limitations in both techniques, spatial heterogeneity, and

497 the oscillations in biomass arising from seasonality. The pattern of microbial abundance observed in

498 the Midtre Lovénbreen forefield broadly resembles that of other glacier forefields worldwide (Insam

499 and Haselwandter, 1989; Bernasconi et al., 2011; Schulz et al., 2013).

500

501 The genomic data indicated that subglacial microbes are dominant in recently exposed soils, in

502 agreement with model results (Fig. 8). The community structure in year 5 was heavily dominated by

503 chemolithoautotrophs (A_1), which reflected findings from previous studies whereby

504 chemolithoautotrophic bacteria contribute to the oxidation of FeS_2 in proglacial moraines in Midtre

505 Lovénbreen (Borin et al., 2010; Mapelli et al., 2011). These processes are also commonly described

506 in other subglacial habitats (Boyd et al., 2014; Hamilton et al., 2013). Based on 16S data, the

507 subglacial community declined in relative abundance with soil age. This finding was also reflected in

508 the model in years 50 and 113. As the age of the soil progressed, there was typically greater

509 abundance of microbes representing typical soil bacteria (groups A_2 and H_2) in the 16S data and the

510 model, thus the relative abundance of subglacial microbes decreased. Microscopy and modelling

511 indicated a predominantly autotrophic community, however 16S data indicated the contrary –

512 especially in the later stages of soil development. Nevertheless, both the 16S and microscopy data

513 indicated that there was a mixed community of autotrophs and heterotrophs in soils of all ages, which

514 was supported by modelling, since no functional groups were extirpated over simulations representing

515 120 years of soil development.

516

517 Nitrogen-fixing bacteria were prevalent in recently exposed soils but declined in relative abundance
518 with soil age. By fixing N_2 instead of assimilating DIN, the model predicted that nitrogen-fixers were
519 able to grow rapidly in the early stages relative to other organisms (Fig. 3a and 3b). The model
520 prediction supports findings by previous studies demonstrating the importance of nitrogen fixation in
521 glacier forefields (Duc et al., 2009; Schmidt et al., 2008; Strauss et al., 2012) and other glacial
522 ecosystems (Telling et al., 2011; Telling et al., 2012). However, there was poor agreement on the
523 relative abundance of nitrogen fixers between the model and the 16S data in the later stages of soil
524 development (years 50 to 120). The model over-predicted the relative abundance of nitrogen fixing
525 organisms (Fig. 8). The majority of the biomass of the autotrophic nitrogen fixers was composed of
526 sequences belonging to the cyanobacterium from the genus *Nostoc*. *Nostoc* forms macroscopically
527 visible colonies that grow on the surface of the soils. Its distribution in the Arctic soils is thus extremely
528 patchy and therefore part of the discrepancy between the 16S data and the model regarding the
529 relative distribution of the A_3 group in the older soils could be due to under-sampling of the *Nostoc*
530 colonies. Allochthonous inputs of nitrogen to the Arctic (e.g. aerial deposition (Geng et al., 2014))
531 strongly affect the productivity of microbial ecosystems and the requirement of nitrogen fixation for
532 microbes (Bjorkman et al., 2013; Kuhnel et al., 2013; Kuhnel et al., 2011; Hodson et al., 2010; Telling
533 et al., 2012; Galloway et al., 2008). Thus, uncertainty in the allochthonous availability of nitrogen
534 strongly affects nitrogen fixation rates. In attempting to replicate a qualitative understanding of the
535 nitrogen cycle in a quantitative mathematical modelling framework, the predicted importance of
536 nitrogen-fixing organisms may be over-estimated. The poor agreement in the relative abundance of
537 nitrogen-fixers between the model and the 16S data indicates an incomplete understanding of
538 allochthonous versus autochthonous nutrient availability. Allochthonous nutrient availability is a known
539 source of uncertainty (Bradley et al., 2014; Schulz et al., 2013; Schmidt et al., 2008), and addressing
540 this concern is the subject of future work.
541
542 **4.3. Net ecosystem metabolism and carbon budget**
543 The seasonality of carbon fluxes predicted by the model (Fig. 4b and 4c) related to the high measured
544 Q_{10} values. High seasonal variation in biotic fluxes and rates is typical of cryospheric soil ecosystems
545 (Schostag et al., 2015) including glacier forefield soils (Lazzaro et al., 2012; Lazzaro et al., 2015).
546 However, microbial activity has been shown to persist during winter under insulating layers of snow
547 and in sub-zero temperatures (Zhang et al., 2014). Modelling also predicted sustained organic
548 substrate degradation, microbial turnover and net heterotrophy during the winter (Fig. 4b and 4c), as
549 documented in other glacier forefield studies (Guelland et al., 2013b), at a low rate.
550
551 The low measured BGE has three important consequences. Firstly, low BGE suggests that a large
552 pool of substrate is required to support heterotrophic growth. Low-efficiency heterotrophic growth lead
553 to the rapid depletion of substrate; therefore high allochthonous inputs were required to maintain a
554 sizeable pool. In older soils (years 80 to 120), increased inputs from microbial necromass (blue line,
555 Fig. 4d) sustained substrate supply to heterotrophs. The sources of allochthonous carbon substrate to
556 the glacier forefield include meltwater inputs derived from the supraglacial and subglacial ecosystems

557 (Stibal et al., 2008; Hodson et al., 2005; Mindl et al., 2007), snow algae (which are known to be

558 prolific primary colonizers and producers in High Arctic snow packs (Lutz et al., 2015; Lutz et al.,

559 2014), atmospheric deposition (Kuhnel et al., 2013) and ornithogenic deposition (e.g. fecal matter of

560 birds and animals) (Jakubas et al., 2008; Ziolek and Melke, 2014; Luoto et al., 2015; Michelutti et al.,

561 2009; Michelutti et al., 2011; Moe et al., 2009). Microbial dynamics are moderately sensitive to

562 external allochthonous inputs of substrate (Bradley et al., 2015), and addressing the uncertainty

563 associated with this flux is an important question to address in future research.

564

565 Secondly, low BGE causes a net efflux of CO_2 over the first 120 years of soil development despite

566 high autotrophic production (Fig. 3e and 3f). Recent literature has explored the carbon dynamics of

567 glacier forefield ecosystems, finding highly variable soil respiration rates (Bekku et al., 2004; Schulz et

568 al., 2013; Guelland et al., 2013a). Future studies should focus on quantifying carbon and nutrient

569 transformations and the potential for forefield systems to impact global biogeochemical cycles in

570 response to future climate change (Smittenberg et al., 2012) and in the context of large-scale ice

571 retreat.

572

573 Thirdly, high rates of substrate degradation encouraged by low BGE were responsible for rapid

574 nutrient release. Modelling suggested that microbial growth was strongly inhibited by low nutrient

575 availability in initial soils (4 µg N g^{-1}, 2 to 10 µg P g^{-1}) (Fig. 3d). This is consistent with findings from

576 the Hailuogou Glacier (Gongga Shan, China) and Damma Glacier (Switzerland) (Prietzel et al., 2013).

577 Low BGE is predicted by the model to have a very important role in encouraging the release of

578 nutrients from organic material more rapidly, thereby increasing total bacterial production in the

579 intermediate stages of soil development. Increased nutrient availability with increased heterotrophic

580 biomass is consistent with recent observations from glacier forefields (Bekku et al., 2004; Schulz et

581 al., 2013; Schmidt et al., 2008).

582

5. Conclusions

584 We used laboratory-based mesocosm experiments to measure three key model parameters:

585 maximum microbial growth rate (I_{max}) (by incorporation of ^{3}H-leucine), BGE (Y) (by measuring

586 respiration rates) and the temperature response (Q_{10}) (by measuring rates at different ambient

587 temperatures). Laboratory-derived parameters were comparable with previous estimations, and

588 refined model predictions by narrowing the range of model output over nominal environmental

589 conditions, thus increasing confidence in model predictions. Our results demonstrated that microbial

590 dynamics at the initial stages of soil development in glacial forefields do not contribute to significant

591 accumulation of organic carbon due the very low growth efficiency of the microbial community,

592 resulting in a net efflux of CO_2 from those habitats. However, the low bacterial growth efficiency in

593 glacial forefields is also responsible for high rates of nutrient recycling that most probably have an

594 important role on the establishment of plants at older ages. The relative importance of allochthonous

595 versus autochthonous substrate and nutrients is the focus of future research.

596

597 Much of the extreme ice-free regions in Antarctica are characterized by a complete absence of higher

598 order plants. However even these environments contain diverse microbial populations and extremely

599 low but detectable levels of organic carbon (Cowan et al., 2014), making these environments suitable

600 cases for modelling using SHIMMER. This exercise shows how an integrated model-data approach

601 can improve understanding and predictions of microbial dynamics in forefield soils and disentangle

602 complex processes interactions to ascertain the relative importance of each process independently.

603 This combined approach explored detailed microbial and biogeochemical dynamics of soil

604 development with the view to obtaining a more holistic picture of soil development in a warmer and

605 increasingly ice-free future world.

606

607 **Acknowledgements**

608 We thank Siegrid Debatin, Marion Maturilli, and Julia Boike (AWI) for support in acquiring

609 meteorological and radiation data, Simon Cobb and James Williams (University of Bristol) for

610 laboratory assistance, and Nicholas Cox and James Wake for assistance in the field and use of the

611 UK Station Arctic Research base in Ny-Ålesund. This research was supported by NERC grant no.

612 NE/J02399X/1 to A. M. Anesio. S. Arndt acknowledges support from NERC grant no. NE/IO21322/1.

613

614

615 **References**

616 ACIA: Arctic Climate Impacts Assessment, Cambridge University Press, Cambridge, 1042,

617 2005.

618 Alves, R. J. E., Wanek, W., Zappe, A., Richter, A., Svenning, M. M., Schleper, C., and Urich, T.:

619 Nitrification rates in Arctic soils are associated with functionally distinct populations of

620 ammonia-oxidizing archaea, Isme J, 7, 1620-1631, 10.1038/ismej.2013.35, 2013.

621 Anderson, S. P., Drever, J. I., Frost, C. D., and Holden, P.: Chemical weathering in the

622 foreland of a retreating glacier, Geochim Cosmochim Ac, 64, 1173-1189, Doi 10.1016/S0016-

623 7037(99)00358-0, 2000.

624 Anesio, A. M., Hodson, A. J., Fritz, A., Psenner, R., and Sattler, B.: High microbial activity on

625 glaciers: importance to the global carbon cycle, Global Change Biol, 15, 955-960, DOI

626 10.1111/j.1365-2486.2008.01758.x, 2009.

627 Anesio, A. M., Sattler, B., Foreman, C., Telling, J., Hodson, A., Tranter, M., and Psenner, R.:

628 Carbon fluxes through bacterial communities on glacier surfaces, Ann Glaciol, 51, 32-40,

629 2010.

630 Bekku, Y. S., Nakatsubo, T., Kume, A., and Koizumi, H.: Soil microbial biomass, respiration

631 rate, and temperature dependence on a successional glacier foreland in Ny-Alesund,

632 Svalbard, Arct Antarct Alp Res, 36, 395-399, 2004.

633 Bernasconi, S. M., Bauder, A., Bourdon, B., Brunner, I., Bunemann, E., Christl, I., Derungs, N.,

634 Edwards, P., Farinotti, D., Frey, B., Frossard, E., Furrer, G., Gierga, M., Goransson, H.,

635 Gulland, K., Hagedorn, F., Hajdas, I., Hindshaw, R., Ivy-Ochs, S., Jansa, J., Jonas, T., Kiczka, M.,

636 Kretzschmar, R., Lemarchand, E., Luster, J., Magnusson, J., Mitchell, E. A. D., Venterink, H.

637 O., Plotze, M., Reynolds, B., Smittenberg, R. H., Stahli, M., Tamburini, F., Tipper, E. T.,

638 Wacker, L., Welc, M., Wiederhold, J. G., Zeyer, J., Zimmermann, S., and Zumsteg, A.:

639 Chemical and Biological Gradients along the Damma Glacier Soil Chronosequence,

640 Switzerland, Vadose Zone J, 10, 867-883, Doi 10.2136/Vzj2010.0129, 2011.

641 Berner, R. A., Lasaga, A. C., and Garrels, R. M.: The Carbonate-Silicate Geochemical Cycle
642 and Its Effect on Atmospheric Carbon-Dioxide over the Past 100 Million Years, Am J Sci, 283,
643 641-683, 1983.
644 Billings, W. D.: Carbon Balance of Alaskan Tundra and Taiga Ecosystems - Past, Present and
645 Future, Quaternary Sci Rev, 6, 165-177, Doi 10.1016/S0277-3791(00)90007-6, 1987.
646 Bjorkman, M. P., Kuhnel, R., Partridge, D. G., Roberts, T. J., Aas, W., Mazzola, M., Viola, A.,
647 Hodson, A., Strom, J., and Isaksson, E.: Nitrate dry deposition in Svalbard, Tellus B, 65, Artn
648 19071
649 Doi 10.3402/Tellusb.V65i0.19071, 2013.
650 Blagodatsky, S. A., Yevdokimov, I. V., Larionova, A. A., and Richter, J.: Microbial growth in
651 soil and nitrogen turnover: Model calibration with laboratory data, Soil Biol Biochem, 30,
652 1757-1764, Doi 10.1016/S0038-0717(98)00029-7, 1998.
653 Borin, S., Ventura, S., Tambone, F., Mapelli, F., Schubotz, F., Brusetti, L., Scaglia, B., D'Acqui,
654 L. P., Solheim, B., Turicchia, S., Marasco, R., Hinrichs, K. U., Baldi, F., Adani, F., and
655 Daffonchio, D.: Rock weathering creates oases of life in a High Arctic desert, Environ
656 Microbiol, 12, 293-303, DOI 10.1111/j.1462-2920.2009.02059.x, 2010.
657 Boyd, E. S., Hamilton, T. L., Havig, J. R., Skidmore, M. L., and Shock, E. L.: Chemolithotrophic
658 Primary Production in a Subglacial Ecosystem, Appl Environ Microb, 80, 6146-6153,
659 10.1128/Aem.01956-14, 2014.
660 Bradley, J. A., Singarayer, J. S., and Anesio, A. M.: Microbial community dynamics in the
661 forefield of glaciers, Proceedings. Biological sciences / The Royal Society, 281, 2793-2802,
662 10.1098/rspb.2014.0882, 2014.
663 Bradley, J. A., Anesio, A. M., Singarayer, J. S., Heath, M. R., and Arndt, S.: SHIMMER (1.0): a
664 novel mathematical model for microbial and biogeochemical dynamics in glacier forefield
665 ecosystems, Geosci. Model Dev., 8, 3441-3470, 10.5194/gmd-8-3441-2015, 2015.
666 Bradley, J. A., Anesio, A., and Arndt, S.: Bridging the divide: a model-data approach to Polar
667 & Alpine Microbiology, Fems Microbiol Ecol, 10.1093/femsec/fiw015, 2016.
668 Bratbak, G., and Dundas, I.: Bacterial Dry-Matter Content and Biomass Estimations, Appl
669 Environ Microb, 48, 755-757, 1984.
670 Brown, S. P., and Jumpponen, A.: Contrasting primary successional trajectories of fungi and
671 bacteria in retreating glacier soils, Mol Ecol, 23, 481-497, Doi 10.1111/Mec.12487, 2014.
672 Caporaso, J. G., Kuczynski, J., Stombaugh, J., Bittinger, K., Bushman, F. D., Costello, E. K.,
673 Fierer, N., Pena, A. G., Goodrich, J. K., Gordon, J. I., Huttley, G. A., Kelley, S. T., Knights, D.,
674 Koenig, J. E., Ley, R. E., Lozupone, C. A., McDonald, D., Muegge, B. D., Pirrung, M., Reeder, J.,
675 Sevinsky, J. R., Tumbaugh, P. J., Walters, W. A., Widmann, J., Yatsunenko, T., Zaneveld, J.,
676 and Knight, R.: QIIME allows analysis of high-throughput community sequencing data, Nat
677 Methods, 7, 335-336, 10.1038/nmeth.f.303, 2010.
678 Cary, S. C., McDonald, I. R., Barrett, J. E., and Cowan, D. A.: On the rocks: the microbiology of
679 Antarctic Dry Valley soils, Nat Rev Microbiol, 8, 129-138, 10.1038/nrmicro2281, 2010.
680 Cowan, D. A., Makhalanyane, T. P., Dennis, P. G., and Hopkins, D. W.: Microbial ecology and
681 biogeochemistry of continental Antarctic soils, Frontiers in microbiology, 5, Artn 154
682 Doi 10.3389/Fmicb.2014.00154, 2014.
683 Darrah, P. R.: Models of the Rhizosphere .1. Microbial-Population Dynamics around a Root
684 Releasing Soluble and Insoluble Carbon, Plant Soil, 133, 187-199, Doi 10.1007/Bf00009191,
685 1991.

Dessert, C., Dupre, B., Gaillardet, J., Francois, L. M., and Allegre, C. J.: Basalt weathering laws and the impact of basalt weathering on the global carbon cycle, Chem Geol, 202, 257-273, DOI 10.1016/j.chemgeo.2002.10.001, 2003.

Duc, L., Noll, M., Meier, B. E., Burgmann, H., and Zeyer, J.: High Diversity of Diazotrophs in the Forefield of a Receding Alpine Glacier, Microbial Ecol, 57, 179-190, DOI 10.1007/s00248-008-9408-5, 2009.

Dyurgerov, M. B., and Meier, M. F.: Twentieth century climate change: Evidence from small glaciers, P Natl Acad Sci USA, 97, 1406-1411, DOI 10.1073/pnas.97.4.1406, 2000.

Edgar, R. C., Haas, B. J., Clemente, J. C., Quince, C., and Knight, R.: UCHIME improves sensitivity and speed of chimera detection, Bioinformatics, 27, 2194-2200, 10.1093/bioinformatics/btr381, 2011.

Ensign, K. L., Webb, E. A., and Longstaffe, F. J.: Microenvironmental and seasonal variations in soil water content of the unsaturated zone of a sand dune system at Pinery Provincial Park, Ontario, Canada, Geoderma, 136, 788-802, DOI 10.1016/j.geoderma.2006.06.009, 2006.

Esperschutz, J., Perez-de-Mora, A., Schreiner, K., Welzl, G., Buegger, F., Zeyer, J., Hagedorn, F., Munch, J. C., and Schloter, M.: Microbial food web dynamics along a soil chronosequence of a glacier forefield, Biogeosciences, 8, 3283-3294, DOI 10.5194/bg-8-3283-2011, 2011.

Filippelli, G. M.: The global phosphorus cycle, Rev Mineral Geochem, 48, 391-425, DOI 10.2138/rmg.2002.48.10, 2002.

Fleming, K. M., Dowdeswell, J. A., and Oerlemans, J.: Modelling the mass balance of northwest Spitsbergen glaciers and responses to climate change, Annals of Glaciology, Vol 24, 1997, 24, 203-210, 1997.

Foereid, B., and Yearsley, J. M.: Modelling the impact of microbial grazers on soluble rhizodeposit turnover, Plant Soil, 267, 329-342, DOI 10.1007/s11104-005-0139-9, 2004.

Follmi, K. B., Hosein, R., Arn, K., and Steinmann, P.: Weathering and the mobility of phosphorus in the catchments and forefields of the Rhone and Oberaar glaciers, central Switzerland: Implications for the global phosphorus cycle on glacial-interglacial timescales, Geochim Cosmochim Ac, 73, 2252-2282, DOI 10.1016/j.gca.2009.01.017, 2009.

Fountain, A. G., Nylen, T. H., Tranter, M., and Bagshaw, E.: Temporal variations in physical and chemical features of cryoconite holes on Canada Glacier, McMurdo Dry Valleys, Antarctica, J Geophys Res-Biogeo, 113, Artn G01s92 Doi 10.1029/2007jg000430, 2008.

Frey, B., Rieder, S. R., Brunner, I., Plotze, M., Koetzsch, S., Lapanje, A., Brandl, H., and Furrer, G.: Weathering-Associated Bacteria from the Damma Glacier Forefield: Physiological Capabilities and Impact on Granite Dissolution, Appl Environ Microb, 76, 4788-4796, Doi 10.1128/Aem.00657-10, 2010.

Frey, B., Buhler, L., Schmutz, S., Zumsteg, A., and Furrer, G.: Molecular characterization of phototrophic microorganisms in the forefield of a receding glacier in the Swiss Alps, Environ Res Lett, 8, Artn 015033 Doi 10.1088/1748-9326/8/1/015033, 2013.

Galloway, J. N., Townsend, A. R., Erisman, J. W., Bekunda, M., Cai, Z. C., Freney, J. R., Martinelli, L. A., Seitzinger, S. P., and Sutton, M. A.: Transformation of the nitrogen cycle: Recent trends, questions, and potential solutions, Science, 320, 889-892, 10.1126/science.1136674, 2008.

731 Geng, L., Alexander, B., Cole-Dai, J., Steig, E. J., Savarino, J., Sofen, E. D., and Schauer, A. J.:
732 Nitrogen isotopes in ice core nitrate linked to anthropogenic atmospheric acidity change, P
733 Natl Acad Sci USA, 111, 5808-5812, 10.1073/pnas.1319441111, 2014.
734 Goransson, H., Venterink, H. O., and Baath, E.: Soil bacterial growth and nutrient limitation
735 along a chronosequence from a glacier forefield, Soil Biol Biochem, 43, 1333-1340, DOI
736 10.1016/j.soilbio.2011.03.006, 2011.
737 Goulden, M. L., Wofsy, S. C., Harden, J. W., Trumbore, S. E., Crill, P. M., Gower, S. T., Fries, T.,
738 Daube, B. C., Fan, S. M., Sutton, D. J., Bazzaz, A., and Munger, J. W.: Sensitivity of boreal
739 forest carbon balance to soil thaw, Science, 279, 214-217, DOI
740 10.1126/science.279.5348.214, 1998.
741 Guelland, K., Esperschutz, J., Bornhauser, D., Bernasconi, S. M., Kretzschmar, R., and
742 Hagedorn, F.: Mineralisation and leaching of C from C-13 labelled plant litter along an initial
743 soil chronosequence of a glacier forefield, Soil Biol Biochem, 57, 237-247, DOI
744 10.1016/j.soilbio.2012.07.002, 2013a.
745 Guelland, K., Hagedorn, F., Smittenberg, R. H., Goransson, H., Bernasconi, S. M., Hajdas, I.,
746 and Kretzschmar, R.: Evolution of carbon fluxes during initial soil formation along the
747 forefield of Damma glacier, Switzerland, Biogeochemistry, 113, 545-561, DOI
748 10.1007/s10533-012-9785-1, 2013b.
749 Hamilton, T. L., Peters, J. W., Skidmore, M. L., and Boyd, E. S.: Molecular evidence for an
750 active endogenous microbiome beneath glacial ice, Isme J, 7, 1402-1412,
751 10.1038/ismej.2013.31, 2013.
752 Hodkinson, I. D., Coulson, S. J., and Webb, N. R.: Community assembly along proglacial
753 chronosequences in the high Arctic: vegetation and soil development in north-west
754 Svalbard, J Ecol, 91, 651-663, DOI 10.1046/j.1365-2745.2003.00786.x, 2003.
755 Hodson, A., Anesio, A. M., Ng, F., Watson, R., Quirk, J., Irvine-Fynn, T., Dye, A., Clark, C.,
756 McCloy, P., Kohler, J., and Sattler, B.: A glacier respires: Quantifying the distribution and
757 respiration CO2 flux of cryoconite across an entire Arctic supraglacial ecosystem, J Geophys
758 Res-Biogeo, 112, Artn G04s36
759 Doi 10.1029/2007jg000452, 2007.
760 Hodson, A., Roberts, T. J., Engvall, A. C., Holmen, K., and Mumford, P.: Glacier ecosystem
761 response to episodic nitrogen enrichment in Svalbard, European High Arctic,
762 Biogeochemistry, 98, 171-184, DOI 10.1007/s10533-009-9384-y, 2010.
763 Hodson, A. J., Mumford, P. N., Kohler, J., and Wynn, P. M.: The High Arctic glacial ecosystem:
764 new insights from nutrient budgets, Biogeochemistry, 72, 233-256, DOI 10.1007/s10533-
765 004-0362-0, 2005.
766 Ingwersen, J., Poll, C., Streck, T., and Kandeler, E.: Micro-scale modelling of carbon turnover
767 driven by microbial succession at a biogeochemical interface, Soil Biol Biochem, 40, 864-878,
768 DOI 10.1016/j.soilbio.2007.10.018, 2008.
769 Insam, H., and Haselwandter, K.: Metabolic Quotient of the Soil Microflora in Relation to
770 Plant Succession, Oecologia, 79, 174-178, Doi 10.1007/Bf00388474, 1989.
771 Jakubas, D., Zmudczynska, K., Wojczulanis-Jakubas, K., and Stempniewicz, L.: Faeces
772 deposition and numbers of vertebrate herbivores in the vicinity of planktivorous and
773 piscivorous seabird colonies in Hornsund, Spitsbergen, Pol Polar Res, 29, 45-58, 2008.
774 Johannessen, O. M., Bengtsson, L., Miles, M. W., Kuzmina, S. I., Semenov, V. A., Alekseev, G.
775 V., Nagurnyi, A. P., Zakharov, V. F., Bobylev, L. P., Pettersson, L. H., Hasselmann, K., and
776 Cattle, A. P.: Arctic climate change: observed and modelled temperature and sea-ice
777 variability, Tellus A, 56, 328-341, DOI 10.1111/j.1600-0870.2004.00060.x, 2004.

778 Kastovska, K., Elster, J., Stibal, M., and Santruckova, H.: Microbial assemblages in soil
779 microbial succession after glacial retreat in Svalbard (high Arctic), Microbial Ecol, 50, 396-
780 407, DOI 10.1007/s00248-005-0246-4, 2005.
781 King, A. J., Meyer, A. F., and Schmidt, S. K.: High levels of microbial biomass and activity in
782 unvegetated tropical and temperate alpine soils, Soil Biol Biochem, 40, 2605-2610, DOI
783 10.1016/j.soilbio.2008.06.026, 2008.
784 Kirchman, D.: Measuring Bacterial Biomass Production and Growth Rates from Leucine
785 Incorporation in Natural Aquatic Environments in: Marine Microbiology, edited by: Paul, J.
786 H., Academic Press, London, UK, 2001.
787 Kirschke, S., Bousquet, P., Ciais, P., Saunois, M., Canadell, J. G., Dlugokencky, E. J.,
788 Bergamaschi, P., Bergmann, D., Blake, D. R., Bruhwiler, L., Cameron-Smith, P., Castaldi, S.,
789 Chevallier, F., Feng, L., Fraser, A., Heimann, M., Hodson, E. L., Houweling, S., Josse, B.,
790 Fraser, P. J., Krummel, P. B., Lamarque, J. F., Langenfelds, R. L., Le Quere, C., Naik, V.,
791 O'Doherty, S., Palmer, P. I., Pison, I., Plummer, D., Poulter, B., Prinn, R. G., Rigby, M.,
792 Ringeval, B., Santini, M., Schmidt, M., Shindell, D. T., Simpson, I. J., Spahni, R., Steele, L. P.,
793 Strode, S. A., Sudo, K., Szopa, S., van der Werf, G. R., Voulgarakis, A., van Weele, M., Weiss,
794 R. F., Williams, J. E., and Zeng, G.: Three decades of global methane sources and sinks, Nat
795 Geosci, 6, 813-823, Doi 10.1038/Ngeo1955, 2013.
796 Knapp, E. B., Elliott, L. F., and Campbell, G. S.: Carbon, Nitrogen and Microbial Biomass
797 Interrelationships during the Decomposition of Wheat Straw - a Mechanistic Simulation-
798 Model, Soil Biol Biochem, 15, 455-461, Doi 10.1016/0038-0717(83)90011-1, 1983.
799 Kuhnel, R., Roberts, T. J., Bjorkman, M. P., Isaksson, E., Aas, W., Holmen, K., and Strom, J.:
800 20-Year Climatology of NO3- and NH4+ Wet Deposition at Ny-Alesund, Svalbard, Adv
801 Meteorol, Artn 406508
802 Doi 10.1155/2011/406508, 2011.
803 Kuhnel, R., Bjorkman, M. P., Vega, C. P., Hodson, A., Isaksson, E., and Strom, J.: Reactive
804 nitrogen and sulphate wet deposition at Zeppelin Station, Ny-Alesund, Svalbard, Polar Res,
805 32, Unsp 19136
806 Doi 10.3402/Polar.V32i0.19136, 2013.
807 Lazzaro, A., Brankatschk, R., and Zeyer, J.: Seasonal dynamics of nutrients and bacterial
808 communities in unvegetated alpine glacier forefields, Appl Soil Ecol, 53, 10-22, DOI
809 10.1016/j.apsoil.2011.10.013, 2012.
810 Lazzaro, A., Hilfiker, D., and Zeyer, J.: Structures of Microbial Communities in Alpine Soils:
811 Seasonal and Elevational Effects, Frontiers in microbiology, 6, ARTN 1330
812 10.3389/fmicb.2015.01330, 2015.
813 Lee, S.: A theory for polar amplification from a general circulation perspective, Asia-Pac J
814 Atmos Sci, 50, 31-43, DOI 10.1007/s13143-014-0024-7, 2014.
815 Luoto, T. P., Oksman, M., and Ojala, A. E. K.: Climate change and bird impact as drivers of
816 High Arctic pond deterioration, Polar Biol, 38, 357-368, 10.1007/s00300-014-1592-9, 2015.
817 Lutz, S., Anesio, A. M., Villar, S. E. J., and Benning, L. G.: Variations of algal communities
818 cause darkening of a Greenland glacier, Fems Microbiol Ecol, 89, 402-414, 10.1111/1574-
819 6941.12351, 2014.
820 Lutz, S., Anesio, A. M., Edwards, A., and Benning, L. G.: Microbial diversity on Icelandic
821 glaciers and ice caps, Frontiers in microbiology, 6, ARTN 307
822 10.3389/fmicb.2015.00307, 2015.
823 Mapelli, F., Marasco, R., Rizzi, A., Baldi, F., Ventura, S., Daffonchio, D., and Borin, S.: Bacterial
824 Communities Involved in Soil Formation and Plant Establishment Triggered by Pyrite

825 Bioweathering on Arctic Moraines, Microbial Ecol, 61, 438-447, 10.1007/s00248-010-9758-
826 7, 2011.
827 McDonald, D., Price, M. N., Goodrich, J., Nawrocki, E. P., DeSantis, T. Z., Probst, A.,
828 Andersen, G. L., Knight, R., and Hugenholtz, P.: An improved Greengenes taxonomy with
829 explicit ranks for ecological and evolutionary analyses of bacteria and archaea, Isme J, 6,
830 610-618, 10.1038/ismej.2011.139, 2012.
831 Michelutti, N., Keatley, B. E., Brimble, S., Blais, J. M., Liu, H. J., Douglas, M. S. V., Mallory, M.
832 L., Macdonald, R. W., and Smol, J. P.: Seabird-driven shifts in Arctic pond ecosystems, P Roy
833 Soc B-Biol Sci, 276, 591-596, 10.1098/rspb.2008.1103, 2009.
834 Michelutti, N., Mallory, M. L., Blais, J. M., Douglas, M. S. V., and Smol, J. P.: Chironomid
835 assemblages from seabird-affected High Arctic ponds, Polar Biol, 34, 799-812,
836 10.1007/s00300-010-0934-5, 2011.
837 Mindl, B., Anesio, A. M., Meirer, K., Hodson, A. J., Laybourn-Parry, J., Sommaruga, R., and
838 Sattler, B.: Factors influencing bacterial dynamics along a transect from supraglacial runoff
839 to proglacial lakes of a high Arctic glacieri (vol 7, pg 307, 2007), Fems Microbiol Ecol, 59,
840 762-762, DOI 10.1111/j.1574-6941.2007.00295.x, 2007.
841 Moe, B., Stempniewicz, L., Jakubas, D., Angelier, F., Chastel, O., Dinessen, F., Gabrielsen, G.
842 W., Hanssen, F., Karnovsky, N. J., Ronning, B., Welcker, J., Wojczulanis-Jakubas, K., and Bech,
843 C.: Climate change and phenological responses of two seabird species breeding in the high-
844 Arctic, Mar Ecol Prog Ser, 393, 235-246, 10.3354/meps08222, 2009.
845 Moreau, M., Mercier, D., Laffly, D., and Roussel, E.: Impacts of recent paraglacial dynamics
846 on plant colonization: A case study on Midtre Lovenbreen foreland, Spitsbergen (79 degrees
847 N), Geomorphology, 95, 48-60, DOI 10.1016/j.geomorph.2006.07.031, 2008.
848 Moritz, R. E., Bitz, C. M., and Steig, E. J.: Dynamics of recent climate change in the Arctic,
849 Science, 297, 1497-1502, DOI 10.1126/science.1076522, 2002.
850 Oechel, W. C., Hastings, S. J., Vourlitis, G., Jenkins, M., Riechers, G., and Grulke, N.: Recent
851 Change of Arctic Tundra Ecosystems from a Net Carbon-Dioxide Sink to a Source, Nature,
852 361, 520-523, DOI 10.1038/361520a0, 1993.
853 Oechel, W. C., Vourlitis, G. L., Hastings, S. J., Zulueta, R. C., Hinzman, L., and Kane, D.:
854 Acclimation of ecosystem CO2 exchange in the Alaskan Arctic in response to decadal climate
855 warming, Nature, 406, 978-981, Doi 10.1038/35023137, 2000.
856 Paul, F., Frey, H., and Le Bris, R.: A new glacier inventory for the European Alps from Landsat
857 TM scenes of 2003: challenges and results, Ann Glaciol, 52, 144-152, 2011.
858 Prietzel, J., Dumig, A., Wu, Y. H., Zhou, J., and Klysubun, W.: Synchrotron-based P K-edge
859 XANES spectroscopy reveals rapid changes of phosphorus speciation in the topsoil of two
860 glacier foreland chronosequences, Geochim Cosmochim Ac, 108, 154-171, DOI
861 10.1016/j.gca.2013.01.029, 2013.
862 Schipper, L. A., Hobbs, J. K., Rutledge, S., and Arcus, V. L.: Thermodynamic theory explains
863 the temperature optima of soil microbial processes and high Q(10) values at low
864 temperatures, Global Change Biol, 20, 3578-3586, Doi 10.1111/Gcb.12596, 2014.
865 Schloss, P. D., Westcott, S. L., Ryabin, T., Hall, J. R., Hartmann, M., Hollister, E. B., Lesniewski,
866 R. A., Oakley, B. B., Parks, D. H., Robinson, C. J., Sahl, J. W., Stres, B., Thallinger, G. G., Van
867 Horn, D. J., and Weber, C. F.: Introducing mothur: Open-Source, Platform-Independent,
868 Community-Supported Software for Describing and Comparing Microbial Communities, Appl
869 Environ Microb, 75, 7537-7541, 10.1128/Aem.01541-09, 2009.
870 Schmidt, S. K., Reed, S. C., Nemergut, D. R., Grandy, A. S., Cleveland, C. C., Weintraub, M. N.,
871 Hill, A. W., Costello, E. K., Meyer, A. F., Neff, J. C., and Martin, A. M.: The earliest stages of

872   ecosystem succession in high-elevation (5000 metres above sea level), recently deglaciated
873   soils, P Roy Soc B-Biol Sci, 275, 2793-2802, DOI 10.1098/rspb.2008.0808, 2008.
874   Schostag, M., Stibal, M., Jacobsen, C. S., Baelum, J., Tas, N., Elberling, B., Jansson, J. K.,
875   Semenchuk, P., and Prieme, A.: Distinct summer and winter bacterial communities in the
876   active layer of Svalbard permafrost revealed by DNA- and RNA-based analyses, Frontiers in
877   microbiology, 6, ARTN 399
878   10.3389/fmicb.2015.00399, 2015.
879   Schulz, S., Brankatschk, R., Dumig, A., Kogel-Knabner, I., Schloter, M., and Zeyer, J.: The role
880   of microorganisms at different stages of ecosystem development for soil formation,
881   Biogeosciences, 10, 3983-3996, DOI 10.5194/bg-10-3983-2013, 2013.
882   Schutte, U. M. E., Abdo, Z., Bent, S. J., Williams, C. J., Schneider, G. M., Solheim, B., and
883   Forney, L. J.: Bacterial succession in a glacier foreland of the High Arctic, Isme J, 3, 1258-
884   1268, DOI 10.1038/ismej.2009.71, 2009.
885   Scott, E. M., Rattray, E. A. S., Prosser, J. I., Killham, K., Glover, L. A., Lynch, J. M., and Bazin,
886   M. J.: A Mathematical-Model for Dispersal of Bacterial Inoculants Colonizing the Wheat
887   Rhizosphere, Soil Biol Biochem, 27, 1307-1318, Doi 10.1016/0038-0717(95)00050-O, 1995.
888   Serreze, M. C., Walsh, J. E., Chapin, F. S., Osterkamp, T., Dyurgerov, M., Romanovsky, V.,
889   Oechel, W. C., Morison, J., Zhang, T., and Barry, R. G.: Observational evidence of recent
890   change in the northern high-latitude environment, Climatic Change, 46, 159-207, Doi
891   10.1023/A:1005504031923, 2000.
892   Simon, M., and Azam, F.: Protein-Content and Protein-Synthesis Rates of Planktonic Marine-
893   Bacteria, Mar Ecol Prog Ser, 51, 201-213, DOI 10.3354/meps051201, 1989.
894   Smittenberg, R. H., Gierga, M., Goransson, H., Christl, I., Farinotti, D., and Bernasconi, S. M.:
895   Climate-sensitive ecosystem carbon dynamics along the soil chronosequence of the Damma
896   glacier forefield, Switzerland, Global Change Biol, 18, 1941-1955, DOI 10.1111/j.1365-
897   2486.2012.02654.x, 2012.
898   Soetaert, K., and Herman, P.: A Practical Guide to Ecological Modelling: Using R as a
899   Simulation Platform, Springer, UK, 2009.
900   Staines, K. E. H., Carrivick, J. L., Tweed, F. S., Evans, A. J., Russell, A. J., Jóhannesson, T., and
901   Roberts, M.: A multi-dimensional analysis of pro-glacial landscape change at Sólheimajökull,
902   southern Iceland, Earth Surface Processes and Landforms, 40, 809-822, 10.1002/esp.3662,
903   2014.
904   Stapleton, L. M., Crout, N. M. J., Sawstrom, C., Marshall, W. A., Poulton, P. R., Tye, A. M.,
905   and Laybourn-Parry, J.: Microbial carbon dynamics in nitrogen amended Arctic tundra soil:
906   Measurement and model testing, Soil Biol Biochem, 37, 2088-2098, DOI
907   10.1016/j.soilbio.2005.03.016, 2005.
908   Stibal, M., Tranter, M., Benning, L. G., and Rehak, J.: Microbial primary production on an
909   Arctic glacier is insignificant in comparison with allochthonous organic carbon input, Environ
910   Microbiol, 10, 2172-2178, 10.1111/j.1462-2920.2008.01620.x, 2008.
911   Strauss, S. L., Garcia-Pichel, F., and Day, T. A.: Soil microbial carbon and nitrogen
912   transformations at a glacial foreland on Anvers Island, Antarctic Peninsula, Polar Biol, 35,
913   1459-1471, DOI 10.1007/s00300-012-1184-5, 2012.
914   Telling, J., Anesio, A. M., Tranter, M., Irvine-Fynn, T., Hodson, A., Butler, C., and Wadham, J.:
915   Nitrogen fixation on Arctic glaciers, Svalbard, J Geophys Res-Biogeo, 116, Artn G03039
916   Doi 10.1029/2010jg001632, 2011.

917 Telling, J., Stibal, M., Anesio, A. M., Tranter, M., Nias, I., Cook, J., Bellas, C., Lis, G., Wadham,
918 J. L., Sole, A., Nienow, P., and Hodson, A.: Microbial nitrogen cycling on the Greenland Ice
919 Sheet, Biogeosciences, 9, 2431-2442, 10.5194/bg-9-2431-2012, 2012.
920 Toal, M. E., Yeomans, C., Killham, K., and Meharg, A. A.: A review of rhizosphere carbon flow
921 modelling, Plant Soil, 222, 263-281, Doi 10.1023/A:1004736021965, 2000.
922 Tscherko, D., Rustemeier, J., Richter, A., Wanek, W., and Kandeler, E.: Functional diversity of
923 the soil microflora in primary succession across two glacier forelands in the Central Alps, Eur
924 J Soil Sci, 54, 685-696, DOI 10.1046/j.1365-2389.2003.00570.x, 2003.
925 Vandewerf, H., and Verstraete, W.: Estimation of Active Soil Microbial Biomass by
926 Mathematical-Analysis of Respiration Curves - Development and Verification of the Model,
927 Soil Biol Biochem, 19, 253-260, Doi 10.1016/0038-0717(87)90006-X, 1987.
928 Yde, J. C., Finster, K. W., Raiswell, R., Steffensen, J. P., Heinemeier, J., Olsen, J.,
929 Gunnlaugsson, H. P., and Nielsen, O. B.: Basal ice microbiology at the margin of the
930 Greenland ice sheet, Ann Glaciol, 51, 71-79, 2010.
931 Yoshitake, S., Uchida, M., Koizumi, H., Kanda, H., and Nakatsubo, T.: Production of biological
932 soil crusts in the early stage of primary succession on a High Arctic glacier foreland, New
933 Phytol, 186, 451-460, DOI 10.1111/j.1469-8137.2010.03180.x, 2010.
934 Zdanowski, M. K., Zmuda-Baranowska, M. J., Borsuk, P., Swiatecki, A., Gorniak, D., Wolicka,
935 D., Jankowska, K. M., and Grzesiak, J.: Culturable bacteria community development in
936 postglacial soils of Ecology Glacier, King George Island, Antarctica, Polar Biol, 36, 511-527,
937 DOI 10.1007/s00300-012-1278-0, 2013.
938 Zelenev, V. V., van Bruggen, A. H. C., and Semenov, A. M.: "BACWAVE," a spatial-temporal
939 model for traveling waves of bacterial populations in response to a moving carbon source in
940 soil, Microbial Ecol, 40, 260-272, 2000.
941 Zhang, X. Y., Wang, W., Chen, W. L., Zhang, N. L., and Zeng, H.: Comparison of Seasonal Soil
942 Microbial Process in Snow-Covered Temperate Ecosystems of Northern China, Plos One, 9,
943 ARTN e92985
944 10.1371/journal.pone.0092985, 2014.
945 Ziolek, M., and Melke, J.: The impact of seabirds on the content of various forms of
946 phosphorus in organic soils of the Bellsund coast, western Spitsbergen, Polar Res, 33, ARTN
947 19986
948 10.3402/polar.v33.19986, 2014.
949 Zumsteg, A., Bernasconi, S. M., Zeyer, J., and Frey, B.: Microbial community and activity
950 shifts after soil transplantation in a glacier forefield, Appl Geochem, 26, S326-S329, DOI
951 10.1016/j.apgeochem.2011.03.078, 2011.
952 Zumsteg, A., Luster, J., Goransson, H., Smittenberg, R. H., Brunner, I., Bernasconi, S. M.,
953 Zeyer, J., and Frey, B.: Bacterial, Archaeal and Fungal Succession in the Forefield of a
954 Receding Glacier, Microbial Ecol, 63, 552-564, DOI 10.1007/s00248-011-9991-8, 2012.
955 Zumsteg, A., Schmutz, S., and Frey, B.: Identification of biomass utilizing bacteria in a
956 carbon-depleted glacier forefield soil by the use of 13C DNA stable isotope probing, Env
957 Microbiol Rep, 5, 424-437, Doi 10.1111/1758-2229.12027, 2013.
958
959
960
961
962
963
964
965
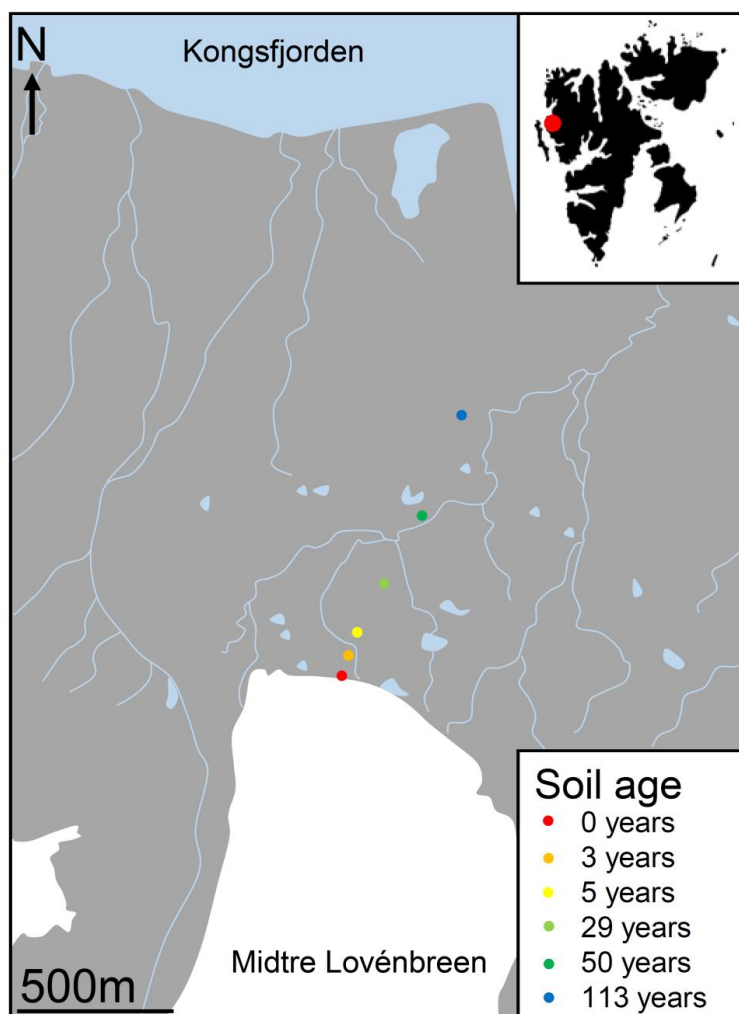
966

967   Figure 1. Midtre Lovénbreen glacier and forefield in Svalbard, the location of sampling sites and

968   approximate age of soil.

969

(a)

(b)

(c)
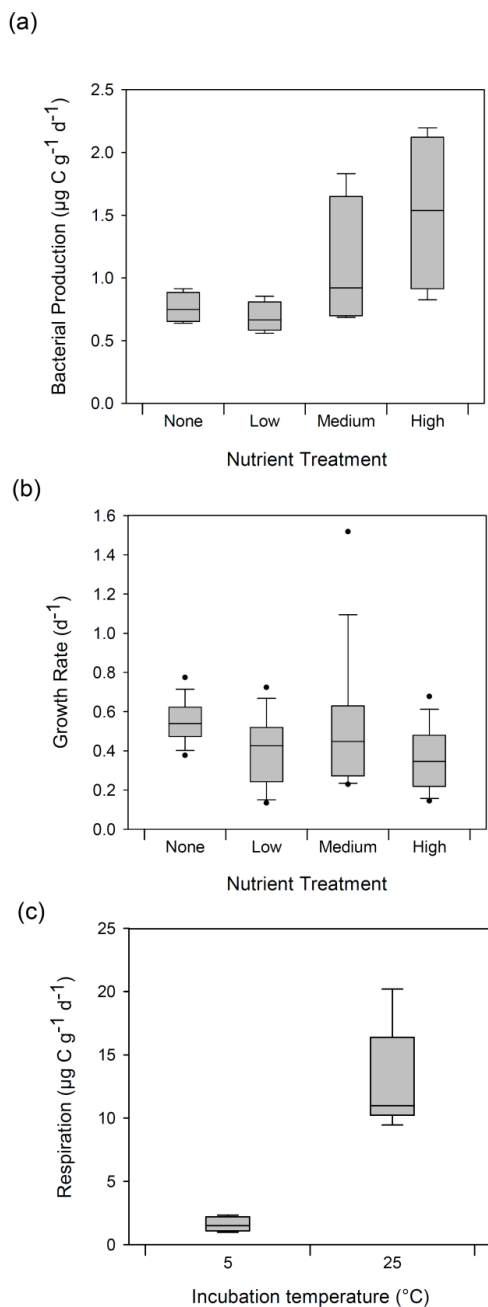
970

971   Figure 2. Measurements of (a) bacterial carbon production and (b) growth rate, derived from ^{3}H-

972   leucine assays at different nutrient conditions, and (c) bacterial respiration at 5˚C and 25˚C.

973

974
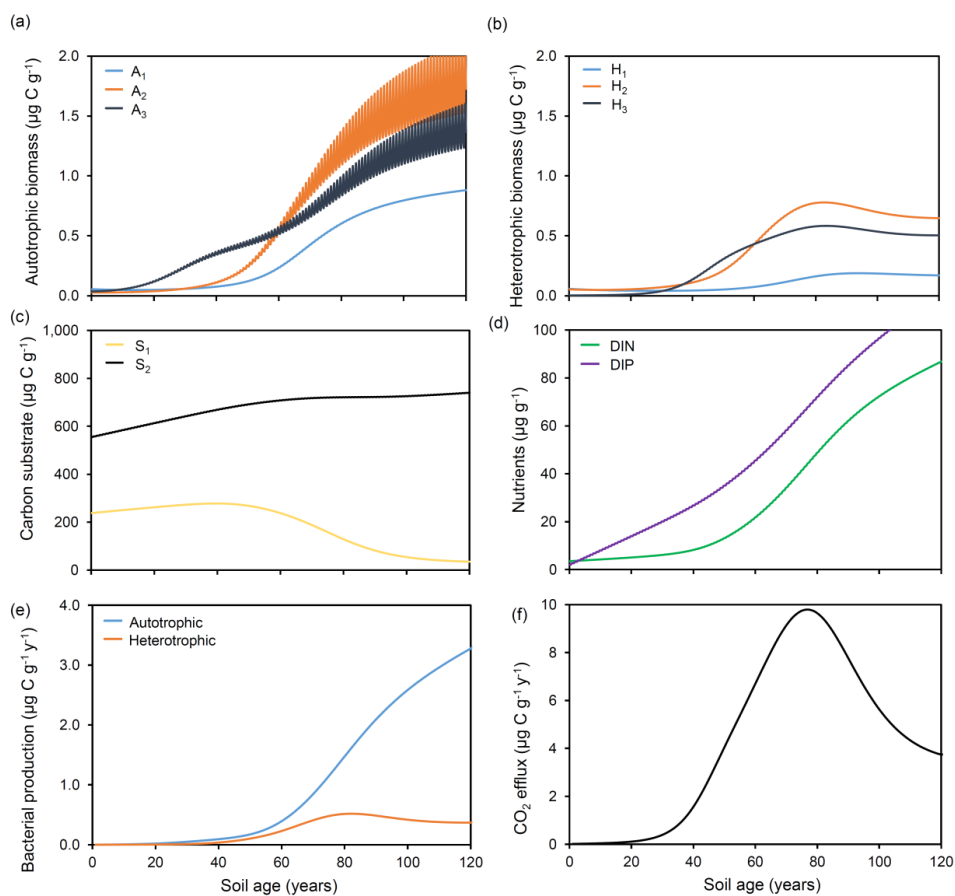
Figure 3. Modelled (a) autotrophic biomass, (b) heterotrophic biomass, (c) carbon substrate, (d) nutrients, (e) bacterial production and (f) CO_2 efflux, with laboratory-derived parameter values.
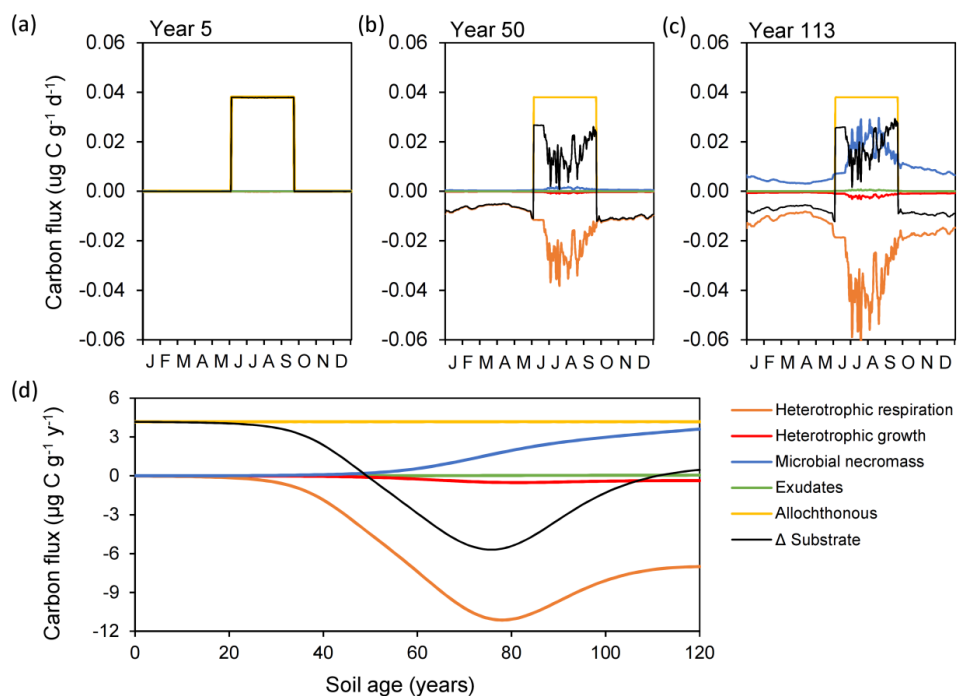
Figure 4. Illustration of daily carbon fluxes for (a) 5, (b) 50 and (c) 113 year old soil, and (d) annual carbon flux over 120 years. Microbial necromass (blue), exudates (green) and allochthonous sources (yellow) contribute to the substrate pool (black), and heterotrophic growth (red) and respiration (orange) deplete it.

985
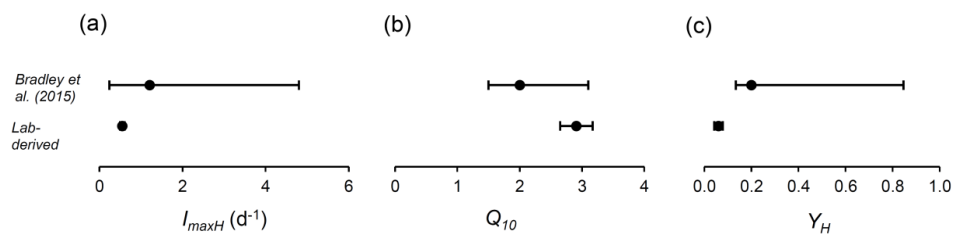
Figure 5. A comparison of previously established ranges for parameters (Bradley et al., 2015) with laboratory-derived values for (a) maximum growth rate (I_{max}), (b) temperature response (Q_{10}), (c) BGE (Y).

989
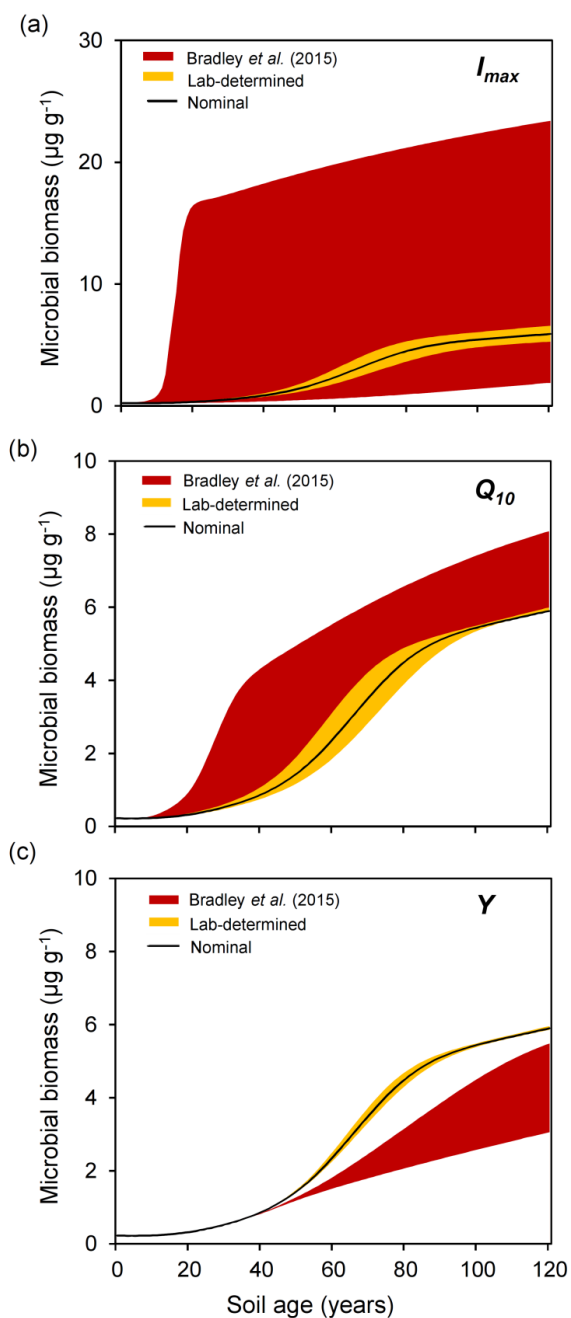
990

991   Figure 6. A comparison of predicted microbial biomass with laboratory-derived parameter values

992   (yellow) and previously established parameter values (Bradley et al., 2015) (red) for variation in the

993   following parameters: (a) maximum growth rate (I_{max}), (b) temperature response (Q_{10}), (c) BGE (Y).

994
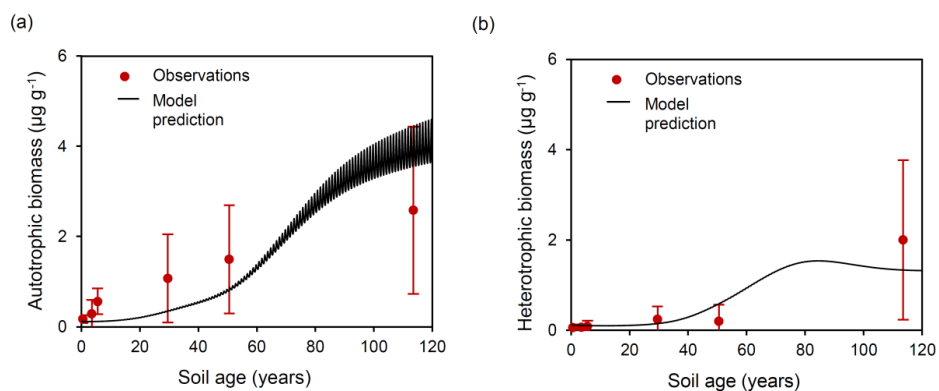
995

996   Figure 7. Model predictions of (a) autotrophic and (b) heterotrophic biomass (black line), compared to

997   observational data (red) derived from microscopy.

998

999
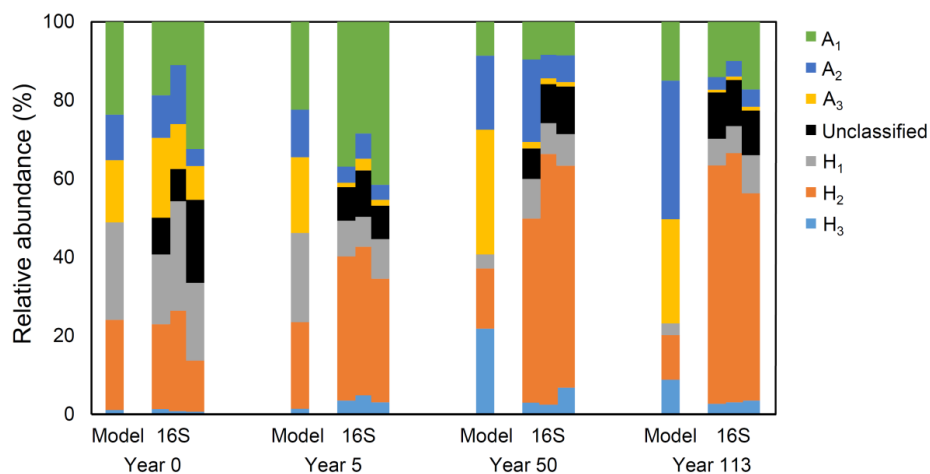
Figure 8. A comparison of microbial diversity from model output and genomic analyses at 0 year old,
5 year old, 50 year old and 113 year old soil.

1000

1001

1002
1003
1004

1005
1006   Table 1. State variables and initial values.

State Variable	Units	Description	Initial value (year 0) ($\mu g\ g^{-1}$)
A_1	$\mu g\ C\ g^{-1}$	Subglacial chemolithoautotrophs	0.0547
A_2	$\mu g\ C\ g^{-1}$	Soil autotrophs	0.0266
A_3	$\mu g\ C\ g^{-1}$	Nitrogen fixing soil autotrophs	0.0355
H_1	$\mu g\ C\ g^{-1}$	Subglacial heterotrophs	0.0576
H_2	$\mu g\ C\ g^{-1}$	Soil heterotrophs	0.0530
H_3	$\mu g\ C\ g^{-1}$	Nitrogen fixing soil heterotrophs	0.0025
S_1	$\mu g\ C\ g^{-1}$	Labile organic carbon	291.895
S_2	$\mu g\ C\ g^{-1}$	Refractory organic carbon	681.089
DIN	$\mu g\ N\ g^{-1}$	Dissolved inorganic nitrogen (DIN)	3.530
DIP	$\mu g\ P\ g^{-1}$	Dissolved inorganic phosphorus (DIP)	2.078
ON_1	$\mu g\ N\ g^{-1}$	Labile organic nitrogen	41.157
ON_2	$\mu g\ N\ g^{-1}$	Refractory organic nitrogen	96.034
OP_1	$\mu g\ P\ g^{-1}$	Labile organic phosphorus	24.227
OP_2	$\mu g\ P\ g^{-1}$	Refractory organic phosphorus	56.530

1007
1008
1009
1010

1011   Table 2. Microbial biomass in the forefield of Midtre Lovénbreen (brackets show 1 standard deviation)
1012

Soil Age (years)	Autotrophic biomass (µg C g^{-1})		Heterotrophic biomass (µg C g^{-1})		Total Organic Carbon (µg C g^{-1})	
0	0.171	(0.042)	0.059	(0.034)	792.984	(127.206)
3	0.287	(0.155)	0.064	(0.029)		
5	0.561	(0.143)	0.083	(0.065)		
29	1.072	(0.487)	0.244	(0.142)		
50	1.497	(0.601)	0.197	(0.184)		
113	2.581	(0.927)	2.000	(0.885)		

1013
1014
1015
1016
1017
1018

1019   Table 3. Model output.

Soil Age (years)	Autotrophic biomass (μg C g^{-1})	Heterotrophic biomass (μg C g^{-1})	Autotrophic production (μg C g^{-1} y^{-1})	Heterotrophic production (μg C g^{-1} y^{-1})	Net CO_2 efflux (μg C g^{-1} y^{-1})	DIN assimilation (μg N g^{-1} y^{-1})	N_2 fixation (μg N g^{-1} y^{-1})
0	0.117	0.111	0.002	0.001	0.011	2.0×10^{-4}	2.0×10^{-4}
3	0.117	0.105	0.003	0.001	0.020	3.0×10^{-4}	3.0×10^{-4}
5	0.119	0.102	0.004	0.001	0.025	4.0×10^{-4}	4.0×10^{-4}
29	0.359	0.147	0.050	0.012	0.391	0.002	0.006
50	0.860	0.591	0.187	0.113	4.311	0.022	0.021
113	4.414	1.331	3.093	0.376	4.031	0.458	0.031

1020
1021
1022
1023
1024
1025
1026